Annex P – MSC SOFTWARE FINAL REPORT

Note: This Annex appears in its original format.

NORTH ATLANTIC TREATY ORGANIZATION

RESEARCH AND TECHNOLOGY ORGANIZATION

AC/323()

www.STO.nato.int

STO TECHNICAL REPORT

Next-Generation NATO Reference Mobility Model (NG-NRMM) Final Report

By MSC Software Corporation

Editors:

Authors: Eric Pesheck, Venkatesan Jeganathan, Tony Bromwell, Aniruddh Matange, Paspuleti Rahul Naidu

Table of Contents

List of Figures

List of Tables

List of Acronyms

MSC	MacNeal-Schwendler Corporation
FED	Fuel Efficient Demonstrator
NATO	North Atlantic Treaty Organization
NRMM	NATO Reference Mobility Model
NG-NRMM	Next Generation NATO Reference Mobility Model
MBD	Multi-Body Dynamics
DEM	Discrete Element Method
CDT	Co-operative Demonstration of Technology
DOF	Degrees of Freedom
Cd	Aerodynamic drag co-efficient
FSD	Frequency Selective damper
AWD	All wheel Drive
PAC	Packeja
AT	Automatic Transmission
COG/CG	Center of Gravity
ADAMS	Automatic Dynamic Analysis of Mechanical Systems
RMS	Root Mean Square
CI	Cone Index
KRC	Keweenaw Research Center
FGW	Fine grain wet sand
ASTM	American Society for Testing and Materials
MP	Mission Profile
FGS	Fine Grain Sand
CGS	Coarse Grain Sand
FG	Fine Grain
UQ	Uncertainty Quantification
VTD	Virtual Test Drive
SIL	Software in Loop
HIL	Hardware in Loop
ADAS	Advanced Driver Assistance Systems
ARB	Anti-Roll Bar
RTI	Real Time Index
RT	Real Time
DLC	Double Lane Change
CRC	Constant Radius Cornering

Final Report of MSC Software Corporation

Next Generation NATO Reference Mobility Model (NRMM) Development

Executive Summary

MSC Software has contributed to the Next Generation NATO Reference Mobility Model (NG-NRMM) by illustrating the capability of current commercial Multi-Body Dynamics analysis tools for predicting military vehicle mobility in a wide variety of scenarios. MSC's Adams™ product suite was used to model the FED-ALPHA (Fuel Efficient Demonstrator) vehicle, successfully validate this model, then accurately predict the vehicle performance on both paved and deformable surfaces. MSC demonstrated capability for incorporating either simplified terramechanics or complex terrramechanics terrain representations into the Adams™ analysis domain and evaluating the corresponding vehicle mobility characteristics.

Additionally, MSC demonstrated the capability to simulate the FED model with Adams™ at real-time speeds, facilitating a variety of autonomous, Driver-in-the-Loop and Hardware-in-the-Loop development scenarios. Lastly, MSC worked with Luciad to demonstrate the capabilities of its geospatial toolset through the creation of a custom application that leveraged the Adams™ simulation results to visualize vehicle mobility characteristics across a specified terrain and predict an optimal cross-country path.

Through this effort, MSC has demonstrated that capable tools and methods are currently available to support extensive prediction of vehicle mobility, and that numerous opportunities exist for integrating these results into complementary applications such as geospatial and autonomous analysis tools.

Chapter 1 – INTRODUCTION

Eric Pesheck
MSC Software Corporation, United States

In support of the Next Generation NATO Reference Mobility Model (NG-NRMM) MSC Software applied its Adams™ Multi-Body Dynamics (MBD) technology to a robust evaluation of the FED-Alpha vehicle mobility. Leveraging prior work, MSC re-built and refined the vehicle dynamics model of the FED-Alpha to an enhanced level of fidelity – upgrading several systems and re-validating the model based on the latest test information.

Upon completion, the vehicle model underwent a series of evaluations in both on- and off-road scenarios, and the results were assessed with respect to the corresponding physical test results. In addition to standard military vehicle criteria, these evaluations included a variety of unique terrain situations and soil types in order to fully comprehend both the model's and the vehicle's range of capabilities. Select results of these evaluations were then integrated into a custom Luciad Lightspeed software application for visualization and mobility mapping.

As part of this thorough evaluation of the vehicle and technology showcase, MSC also leveraged Discreet Element Methods (DEM) for soft soil terramechanics and coupled the corresponding EDEM model with the validated Adams™ model via co-simulation to better represent the vehicle's performance under various soil type and moisture conditions.

Finally, with autonomous vehicles on the horizon, MSC took advantage of the opportunity to showcase its latest capabilities in the area of real-time dynamics. In this effort, a real-time version of the FED vehicle dynamics model was created and verified against the original Adams™ model. To demonstrate its capabilities, MSC installed this model on our driving simulator and made this available for CDT-participant review.

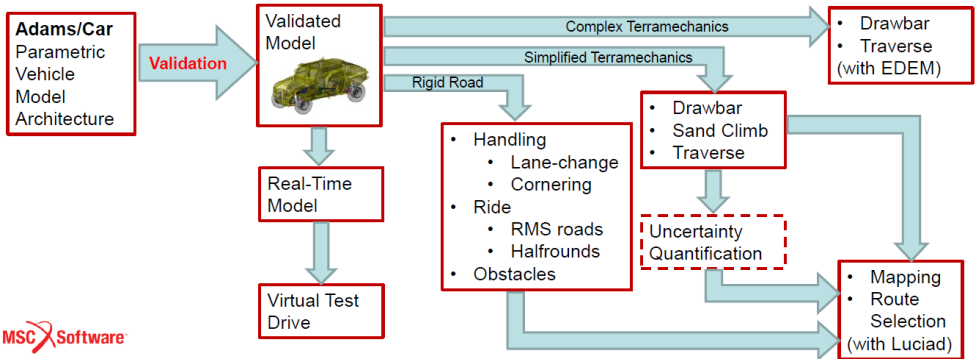

Figure 1-1: MSC AVT-308 Activities Overview

Chapter 2 - Next Generation NATO Reference Mobility Model Modelling

Eric Pesheck, Venkatesan Jeganathan, Aniruddh Matange
MSC Software Corporation, United States

2.1. Introduction to Vehicle Modelling

There are many different types of vehicle models, each meant for a specific purpose. The system elements or components of the vehicle model govern its behavior and appropriate applications. For example, a quarter-car model (one or two degrees of freedom (DOF) vertical model) can be used for simple studies of vertical suspension dynamics, such as active suspension development. Alternatively, a larger 14DOF model is more suitable for basic roll dynamics studies. There are other detailed multibody vehicle models available within commercial software packages with more than 100 DOF. The degree of detail required within the model is determined by the application.

Adams™ is the world's most widely used multibody dynamics simulation software. It lets users build and test realistic virtual prototypes of full-motion complex mechanical system designs. These models can be accurately simulated on standard computer workstations, allowing users to better understand their performance both visually and mathematically. Adams™ has general capabilities for modeling a vast array of mechanical systems, most often in the range of 20-2000 DOF, including disparate applications such as tracked vehicles, chainsaws, escalators, transmissions, wind turbines and drill strings.

Adams™ provides a robust solution engine to solve the mechanical system models. The software checks the model and automatically formulates and solves the equations of motion for kinematic, static, quasi-static, or dynamic analysis conditions. For some applications, Adams™ can automatically iterate through design variables to achieve optimal system performance.

Adams™ Car is a sophisticated product within the Adams™ product family for accurately modeling complete vehicle subsystems, and assumes the user has at least a basic working knowledge of typical vehicle systems. This knowledge is leveraged to build, assemble, and test vehicle models in Adams™ Car. A brief overview including terminology and summaries of Adams™ Car subsystems is provided here for introductory purposes.

As in a real vehicle, an Adams™ Car model consists of multiple subsystems, of which many are predefined in the software. Most, but not all, are required when attempting to run full-vehicle simulations. Typical subsystems used in Adams™ Car full-vehicle models are

- Vehicle Chassis
- Wheel and Tires
- Powertrain
- Suspensions
- Steering
- Brakes

Within the Adams™ Car modelling environment, each subsystem references a corresponding customizable parametric modelling template. This template codifies the subsystem topology, corresponding modeling methods, associated hardpoints, and required parameters. This approach facilitates a modular,

reusable modelling strategy and encourages consistent models both between vehicle variants and within the vehicle analysis organization.

Once populated with vehicle data, the subsystems are integrated to create a full vehicle assembly. After validation of the vehicle model, additional studies on handling, ride, and off-road performance of the vehicle may be carried out and compared with vehicle test measurements.

Select details from each Adams™ Car subsystem are described below:

2.2. Chassis

A vehicle chassis is the underlying structure, often made of steel, upon which the remaining parts and systems of the vehicle are built. Most military vehicles utilize a monocoque or unibody design where the chassis is integrated and assembled with the body of the vehicle.

Most, but certainly not all simulations in Adams™ Car are performed assuming only rigid body mechanics with the exceptions for bushings, springs, dampers, and tire models. All other components, such as the chassis, are not allowed to deform. In the case of real unibody designs, the chassis flexes very little in normal driving events. For this vehicle, the chassis was modelled as rigid body. If warranted, Adams™ does allow for the use of finite-element based flexible bodies. For Adams™ Car models, the mass and inertia properties of the vehicle chassis include all parts mounted to the body and not associated with other subsystems. For instance, all body panels, interior components, wiring, fuel, armor, etc. must be included in the mass properties of the chassis.

The aerodynamic drag effect is considered in the Adams™ model and is applied as a concentrated effective aerodynamic force on the vehicle body. The force takes frontal area, air density and drag co-efficient as inputs to calculate the aerodynamic forces. The FED-Alpha vehicle had a vehicle frontal area of 3.8 m^2 and the drag co-efficient (Cd) of 0.6.

Figure 2-2: FED-Alpha Vehicle Chassis

2.3. Suspension System

The vehicle used for this study uses a double-wishbone suspension design with air springs for both the front and rear suspensions. Modelling of the suspension system started with specifying the hard points.

The hard point coordinates for front suspension are as per Table 2-1, these points belong to the left side of the suspension. As the suspension is symmetrical about the vertical center-plane of the vehicle, the right-side hard points are simply a mirror (a change of sign in the y-coordinate) of these values.

Table 3-1: Front Suspension Hardpoints

LEFT SIDE HARD POINTS			
Front	X	Y	Z
ARB_bushing	770.80	-265.00	699.72
ARB_droplink_lower	1046.75	-588.32	543.34
ARB_droplink_upper	1046.06	-589.19	713.77
Brake_caliper_attachement_1	1113.58	-916.50	611.6
Brake_caliper_attachement_2	1211.06	-916.50	879.4
Brake_caliper_centre_pressure	1115.00	-953.50	762.73
damper_bush_ori_z	1048.89	-493.38	1275.90
drive_shaft_inr	1263.77	-281.20	731.00
drive_shaft_outer	1264.00	-825.41	708.50
lca_front	984.06	-219.00	605.80
lca_outer	1258.33	-858.20	546.26
lca_rear	1568.92	-219.00	638.03
lwr_damper_mount	1145.86	-650.44	608.67
lwr_spring_seat	1145.86	-650.44	608.67
tierod_inner	1486.00	-380.99	820.27
tierod_outer	1465.00	-820.00	780.00
uca_front	1125.00	-294.00	995.25
uca_outer	1272.56	-775.81	953.85
uca_rear	1439.00	-294.00	995.25
upr_damper_mount	1148.80	-498.19	1255.46
upr_spring_seat	1148.89	-493.38	1275.90
wheel_center	1264.00	-976.50	708.50

Similar hardpoints are used to define the rear suspension. In addition, the mass properties (mass, CG location, and inertia properties) for all suspension parts are defined as well. The details of all “standard” model content such as hardpoints and mass properties are not further documented in this report, for the sake of brevity.

For a typical vehicle-dynamics model, the transmission of forces from the wheels to the body is governed by the suspension. The force transmitted is influenced by the kinematic and dynamic components of the suspension system such as links, springs and dampers. The term double wishbone is used to describe any suspension composed of independent, upper and lower control arms suspended by a coil spring and controlled by a damper, as shown in Figure 1.

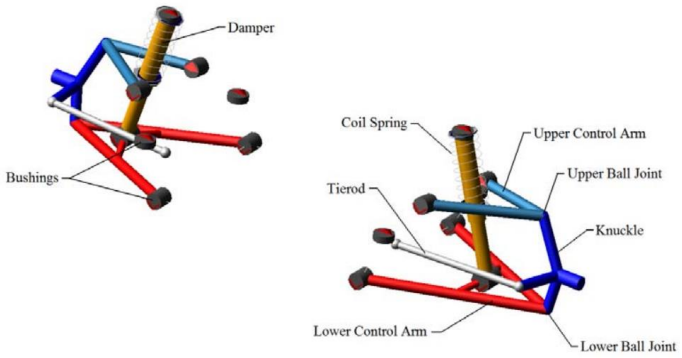

Figure 2-2: Suspension Topology

The upper and lower control arms (A-arms) attach at inner joints to the chassis, via pliable bushings. Outer joints on the control arms control the knuckle, where the brake and wheel are mounted. All driving forces are transmitted to the chassis through the control arms, tie rod and strut forces.

Adams™ Car models air springs as simple action-reaction forces between two parts. The air spring component model references a property file that tabulates spring force against trim load and deflection from trim length. Trim load is the nominal load in the spring for a given trim length and internal pressure. During analysis, Adams™ Solver computes the air-spring force by interpolating the 3D spline data to determine spring force based on current trim load and spring deflection. Below, the measured data (Figure 2-3) and corresponding Adams™ air spring input curves (Figure 2-4) are shown:

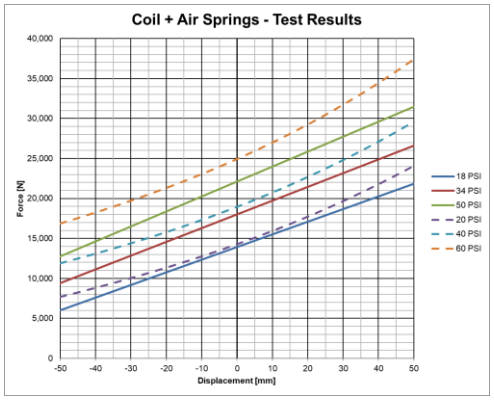

Figure 2-3: Measured Air Spring Characteristics

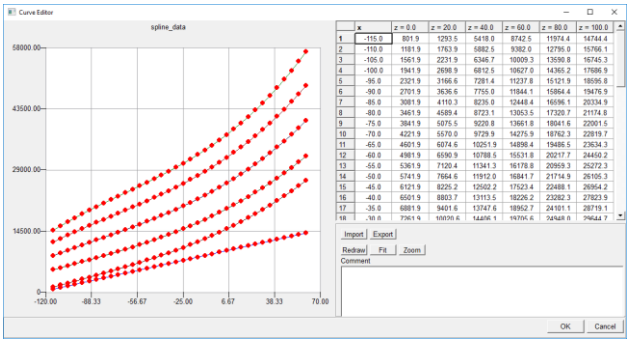

Figure 2-4: Adams™ FED Air Spring Characteristics

The FED-Alpha vehicle uses a Frequency Selective Damper (FSD). It is important to model the FSD damper based on its actual behavior at low and high frequency. The damper forces are determined by force-velocity lookup tables at low and high frequency. In this damper, the frequency-dependent behavior was active only in the rebound condition. Although MATLAB models were provided, the FSD was modelled within Adams™ using run-time measurements and transfer functions to avoid the complications and high computation efforts associated with MATLAB co-simulation. The outputs of the Adams™ FSD were validated against the MATLAB model outputs, as seen below.

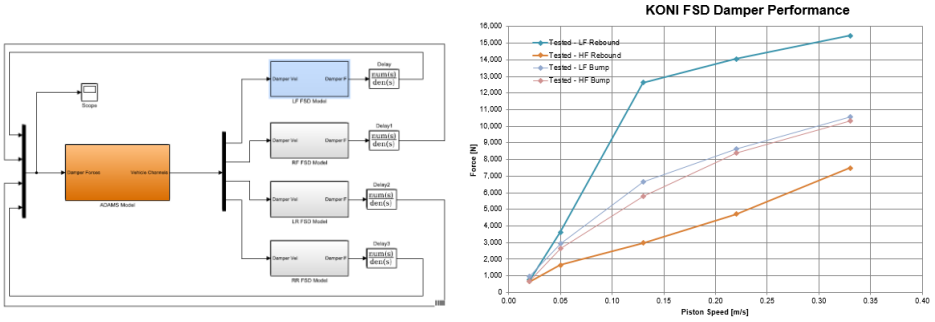

Figure 2-5: FSD Damper Curve

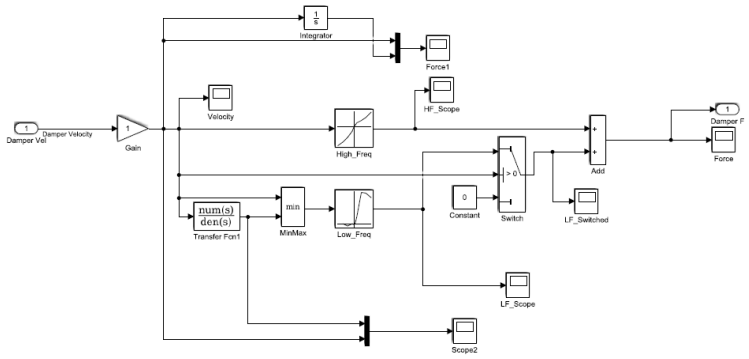

Figure 2-6: FSD Damper Characteristics

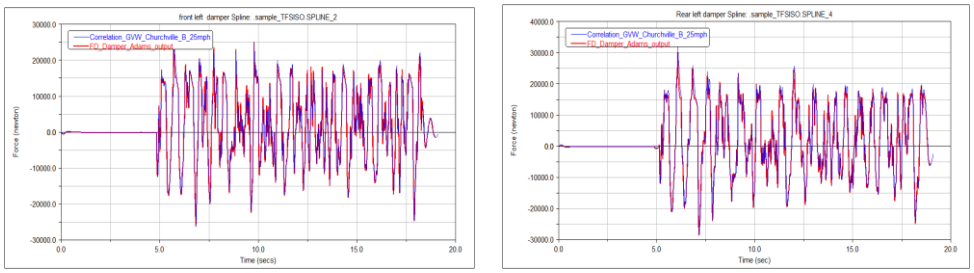

Figure 2-7: Adams™ FSD Damper Force Validation with MATLAB outputs

The front suspension subsystem also incorporates an anti-roll bar, with links to the lower control arms and bushing mounts to the vehicle chassis. Primarily, this element was modelled with a series of beam elements to most accurately capture the added system roll stiffness throughout the model's range of motion. However, for the Real-Time model variant (see Chapter 8), the anti-roll bar was simplified to use rigid parts connected by a central torsional spring.

2.4. Steering System

No vehicle can be properly controlled without a steering subsystem. The steering system must link the front two wheels, maintain a proper amount of toe, and produce correct steer angles when corning. Some common steering mechanisms are rack and pinion or a pitman arm. The vehicle used for this study is equipped with a pitman arm steering mechanism. A steering gear transmits driver inputs from the steering column to the Pitman arm, which rotates through an arc to move the draglink and tie rods. Each tie rod attaches to a knuckle to actuate the steering.

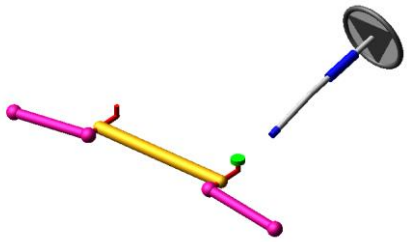

Figure 2.8: Pitman Arm Steering system

As with the suspension subsystems, the steering hardpoints are parameterized for easy model revision and re-use. For this investigation, MSC developed both a compliant steering system with hydraulic boost capability, and a simpler kinematic system without power assist. For most applications, the simpler kinematic system was used to minimize unnecessary complication.

2.5. Powertrain

Propelling a vehicle forward requires the generation and transmission of power. These duties are handled by the powertrain which typically consists of an internal combustion engine, torque converter, transmission, transfer case, and differentials (along with corresponding shafts and joints).

The FED- Alpha vehicle has an AWD configuration with a transfer case that splits the torque generated to the front and rear axles. Half shafts transfer power from a central differential to the wheels in front and rear axle.

The Adams™ engine model consists of a single rigid part representing the total mass and inertia of the engine block, clutch housing, and transmission. A spline representing the engine's steady-state torque versus engine speed and throttle position is used as a lookup table to find the appropriate torque for driving the vehicle. The plots below show the engine power map.

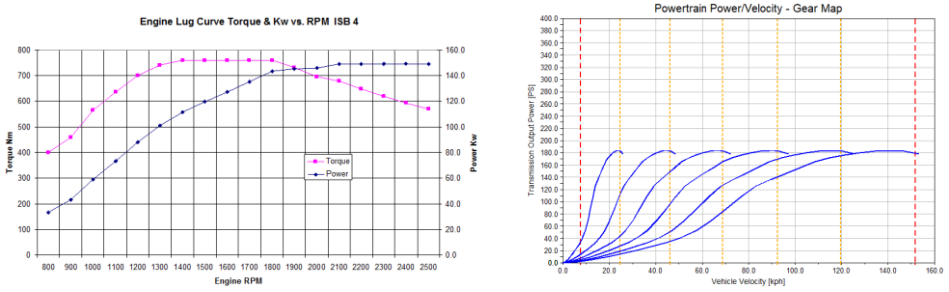

Figure 2-9: Engine Torque Characteristics

The Adams™ transmission model is a simplified model with no rotating inertia. A built-in controller is provided to select the proper gear depending on the engine speed and the shift points specified. The model shifts from the old to the new gear ratio when the input speed reaches the corresponding shift point. The

torque output from the transmission is continuous and approximates the engagement/disengagement of clutches in a real automatic gearbox.

Table 2-2: Transmission Gear Ratios

	Gear [3]	Ratio	Efficiency
Transmission Gear Ratios (individual)	1	3.74	0.91
	2	2.003	0.92
	3	1.343	0.925
	4	1	0.93
	5	0.773	0.925
	6	0.634	0.92
Transfer Case Gear Ratios (individual)	Gear	Ratio	Efficiency
	LOW	2.72	0.944
	HIGH	1.00	0.99

The torque converter component model in Adams™ uses the provided capacity factor and torque ratio curves to calculate appropriate engine drag and downstream torque.

Table 2-3: Torque Converter characteristics

Speed Ratio	Capacity factor[deg/s /(Nm)^0.5]	Speed Ratio	Torque Ratio
-5	503.4	-5	1.747
-2	503.4	-2	1.747
-1	503.4	-1	1.747
0	503.4	0	1.747
0.121	496.2	0.121	1.65
0.242	494.4	0.242	1.574
0.365	492.6	0.365	1.481
0.484	495	0.484	1.386
0.599	499.8	0.599	1.294
0.708	507.6	0.708	1.205
0.787	533.4	0.787	1.127
0.848	565.2	0.848	1.065
0.874	583.2	0.874	1.035
0.895	602.4	0.895	1.009
0.91	625.2	0.908	1.009
0.917	653.4	0.914	1.009
0.924	681.6	0.918	1.009
0.93	709.8	0.922	1.009
0.935	737.4	0.926	1.009
0.94	766.2	0.93	1.009
0.944	795.6	0.934	1.009
0.947	823.8	0.937	1.007
0.949	853.8	0.94	1.007
0.951	882.6	0.943	1.007
0.953	910.8	0.945	1.007
0.956	939.6	0.948	1.007
0.958	967.8	0.95	1.007
0.96	996.6	0.953	1.006
0.962	1026.6	0.955	1.006
0.964	1055.4	0.957	1.004
0.965	1084.8	0.959	1.004
0.996	3240	0.961	1.004
0.997	12960	0.963	1.004
0.998	91000	0.965	1.004
1.001	91000	0.996	1.004
1.004	12960	0.997	1.004
1.006	3240	0.998	1.004
1.013	2000	0.999	1.004
1.019	1800	1.001	1.006
1.025	1350	1.006	1.005
1.1	890	1.013	1.005
1.15	600	1.019	1.005
2	520	1.02	1.005
4	515	1.025	1.005
6	510	1.032	1.0047
8	500	1.052	1.0045
		1.1	1.0043
		1.208	1.0042
		1.258	1.0041
		1.328	1.004
		1.423	1.004
		1.592	1.004
		1.808	1.004
		2.166	1.004
		2.833	1.004
		4.172	1.004
		8.283	1.004

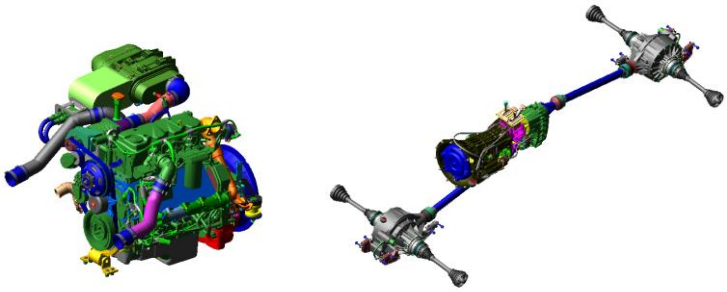

Figure 2-10: Powertrain and Driveline system

2.6. Wheels, Tires and Brakes

The vehicle wheels are treated as rigid parts that are fixed to the rotating spindles in the suspension subsystems. The tire forces then act between the road surface and the wheel part. The tires are vital components for vehicle modeling since tires transmit forces from the ground to the vehicle and vice versa. Adams™ provides a choice of various road and tire models to be used for desired applications. Some examples of available tire models in Adams™ are Fiala, UA, Packeja, Delft, and Ftire.

The FED-Alpha uses a tire of specification 335/65R22.5, width of section 335mm, outside radius 505.46mm, loaded radius of 464.82 mm, and a load capability of 3075 kg. Relevant parameters for the Packeja 2002 (PAC2002) model and a corresponding tire property file were provided and used for all vehicle simulations (with the exception of EDEM co-simulations).. Ideally, an Ftire model would capture the tire behavior with greater accuracy, especially over obstacles, but at a significant computational cost. However, appropriate data to support this approach was not available for this analysis effort.

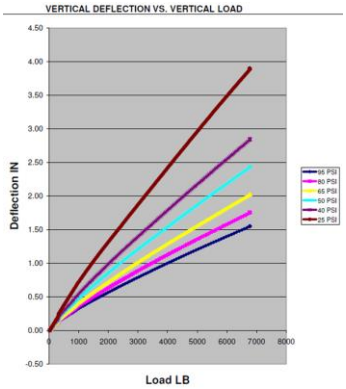

Figure 2-11: Tire Vertical Characteristics

The Brake system in the model consists of torques that are applied between the wheel and the knuckle, driven by the driver brake demand and opposing the wheel velocity. The mass properties of the caliper and rotor are assumed to be integrated into the knuckle and wheel, respectively. For this model, the requirements for brake analysis were minimal and the default Adams™ Car brake system was used. No significant brake component details were incorporated.

2.7. Summary

Adams™ Car models are constructed in much the same way as real vehicles. Individual subsystems are assembled together to create a complete vehicle model. The choice of suspension geometry, mass properties, spring rates and damper rates all can have a profound impact on the characteristics of the model. Thus great care is required to create a meaningful model capable of producing useful results.

Table 2-4: Vehicle Configuration Summary

Wheel base	4648.2 mm
Track width	2286 mm
Unloaded weight	5485 kg
Front suspension	SLA Suspension with Integrated Air-Spring, Frequency selective damper
Rear suspension	SLA Suspension with Integrated Air-Spring, Frequency selective damper
Steering	Pitman Arm
Powertrain	4.5L, 200 hp turbocharged
Driveline	AT, 4WD T-case : high/low gear ratio
Tire size	335/65R22.5

Assumptions:

(i) The vehicle chassis is modelled as a rigid body
(ii) Suspension components are considered to be rigid bodies

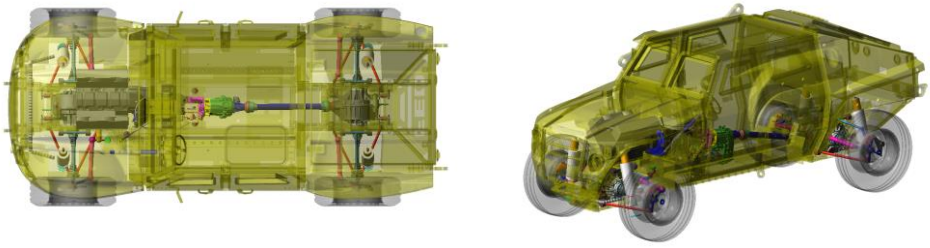

Figure 2-12: Assembled Full Vehicle Model

Chapter 3 - Next Generation NATO Reference Mobility Model Validation

Eric Pesheck, Venkatesan Jeganathan
MSC Software Corporation, United States

Today, most vehicle manufacturers use full-vehicle CAE models in advanced simulations to predict and evaluate the vehicle performance. Only an accurate full-vehicle model can be used to predict the vehicle behavior across numerous types of situations, including handling, ride, durability and mobility. For effective use of a model across these applications, there must be high confidence in its accuracy.

This chapter presents the prediction and correlation of several FED full-vehicle results with Adams™ Car. For the NG-NRMM analysis effort, several test results were selected to use for model validation. Once validated, the model could be used to predict results for numerous additional vehicle test events.

The following metrics and tests were selected for use in the validation stage:

- Weights & COG Calibration
- Steering behavior
  - Steering ratio test
  - Wall to wall turn radius
  - Steady State cornering
- Longitudinal Dynamics
  - Acceleration
  - Braking
- Lateral Dynamics
  - Lane Change (single-speed, 20 mph)
- Ride Quality
  - Half rounds (10” only)
  - RMS Course (2” rms only)
- Traction
  - Drawbar pull

The corresponding model validation results are listed in the following sections.

3.1.Weights & COG Calibration

The aim of this work is to build the multibody model of the FED-alpha with same weight distribution as the test prototype vehicle. The overall CG of the vehicle is adjusted to test configuration and the weight distribution on the axles are achieved. The weight measured on each tire contact patch were compared with the test measurements and found to be close. The weight and CG of the model are presented in Table 3-1

Table 3-1: Weights Summary

	Test	Adams™
Front Left (lb)	3125	3142.25
Front Right (lb)	3135	3085.35
Rear Left (lb)	2965	2958.38
Rear Right (lb)	2860	2901.49

Long CG (in)	62.66	62.63
Lat CG (in)	-0.35	-0.3533

3.2.Steering Behavior

3.2.1. Steering Ratio Test:

The steering ratio test is performed by rotating the hand steering wheel and measuring the steer angle of the road wheel. This test is used to measure the ratio of hand wheel angle to road wheel angle. Figure 3-1 shows the plot of hand wheel angle versus the road wheel angle of the model. The steering wheel ratio from the plot given by the slope of the plot compares well with the test values. This test validates the steering system kinematics of the model.

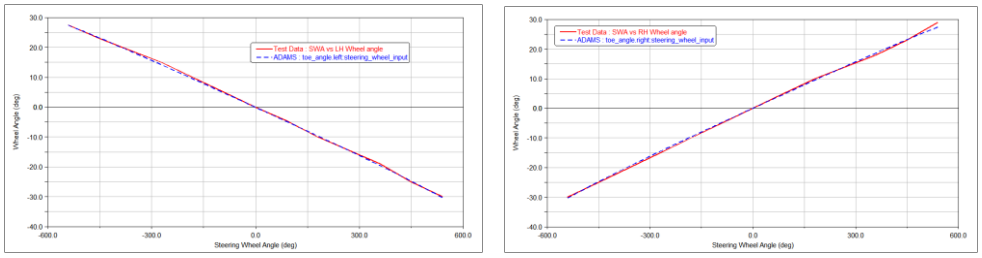

Figure 3-1: Steering Wheel angle versus road wheel angle for Adams™ and Test results

3.2.2. Wall to Wall Turn Radius:

This event is intended to determine the minimum radius for achieving a slow-speed vehicle rotation. This is achieved by slowly driving the vehicle at maximum steering until the vehicle makes one complete rotation. The event is to be performed for both turning directions. For this event, a flat paved road and a friction of 0.93 was used. The speed was maintained at 10 Kph. Estimated coordinates for the outermost corners of the vehicle were selected from the CAD geometry, resulting in a width of 89.8 in (2280.92 mm) and length of 183 in (4648.2 mm)

Prior to analysis, markers were placed at the vehicle corners in order to facilitate tracing the motion in post processing. The primary results required are the positions of the four vehicle corners over the course of the maneuver. This data can be processed to analytically determine the turning radius (see below) and, for graphical purposes, these motions are traced to provide a visual indication of the radius.

The traced paths of the four corners, corresponding to a right-turn spin, are shown in the figure below:

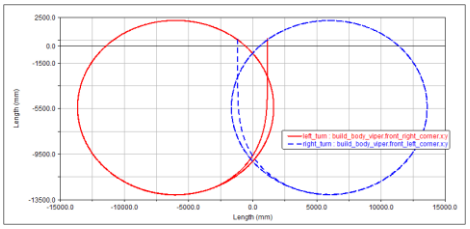

Figure 3-2: Outermost Traced Path of Vehicle

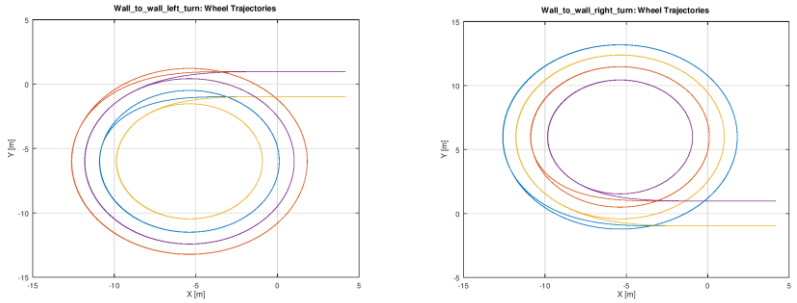

Figure 3-3: Traced Path of Vehicle corners

After processing the curve data shown above, the minimum attainable turn diameter was found as in the table below. This result shows good correlations with test.

Table 3-2: Wall to wall Turn Diameter

Wall to Wall Turn Diameter		
Direction	Test (ft)	Simulation(ft)
CW	51.1	50.11
CCW	50.8	50.25

3.2.3. Steady State Cornering:

The Steady state cornering event consists of traveling a circular path with increasing speed until loss of traction or vehicle control limits the vehicle speed. The path radius is 100 ft (30.48 m), and the vehicle is to start at 5 mph (8.05 kph) and increase speed with steady acceleration such that stability loss occurs. The test is to be performed for both a left and right turn.

In Adams™, for constant-radius cornering analysis, the Driving Machine drives the full vehicle along a circular path on a skidpad, and then gradually increases velocity to build up lateral acceleration. One common use for a constant radius cornering analysis is to determine the understeer characteristics of the full vehicle. The model, with skidpad road and target circular path is shown below:

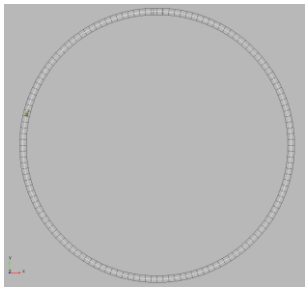

Figure 3-4: Skidpad Road and circular path, Steady State Cornering Event

For this analysis, the primary outputs of interest are the maximum attainable speed, steering wheel angle, roll angle, yaw angle and lateral acceleration.

The primary result of interest are shown in the plots below. The simulation was run using turns in both directions. These generated consistent results with the test measured data.

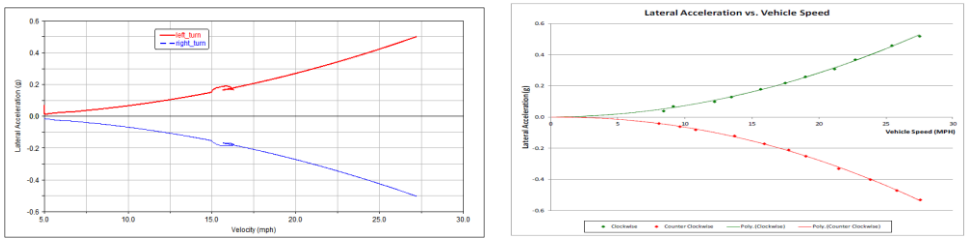

Figure 3-5: CRC : Lateral acceleration vs. Vehicle Speed. Adams™ (left) versus test (right)

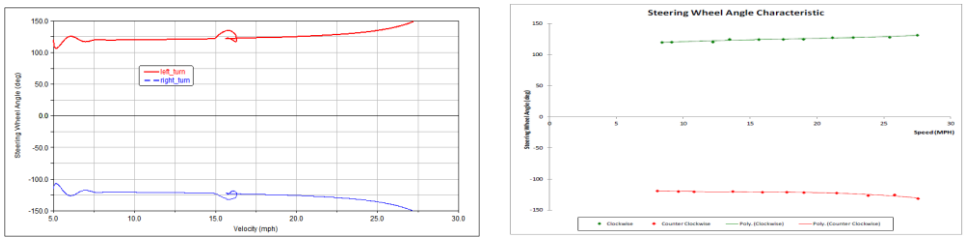

Figure 3-6: CRC : Steering Wheel Angle (SWA) vs. Vehicle Speed. Adams™ (left) versus test (right)

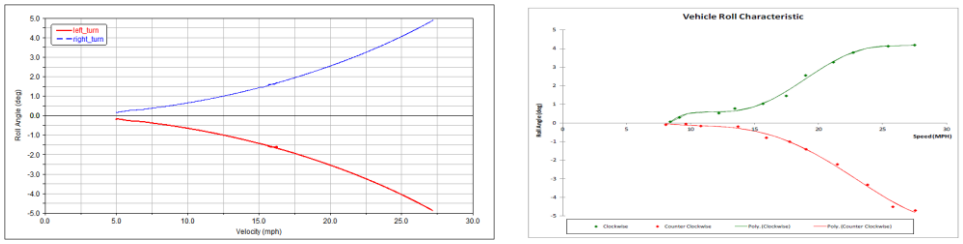

Figure 3-7: CRC : Roll Angle vs. Vehicle Speed. Adams™ (left) versus test (right)

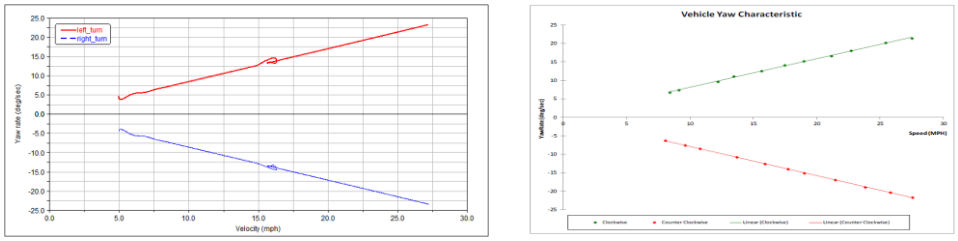

Figure 4-8: CRC : Yaw Angle vs. Vehicle Speed. Adams™ (left) versus test (right)

3.3.Longitudinal Dynamics

3.3.1. Acceleration :

The objective of this test is to determine the operating characteristics of the vehicle under maximum speed and acceleration condition on paved road surface with friction co-efficient of 0.93. Both the physical test and the simulation used applicable portions of TOP 2-2-602 as a general guide for this event.

In Adams™, during an acceleration analysis, the Driving Machine ramps the throttle demand from 0 to 100% over a specified interval of time. For this analysis, the primary results of interest are the longitudinal acceleration, vehicle speed, distance travelled.

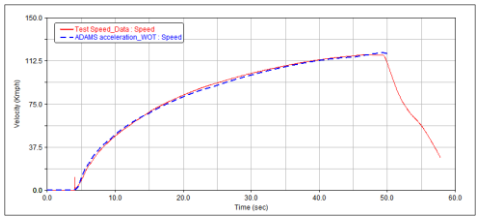

Figure 3-9: Acceleration : Vehicle Speed vs. Time

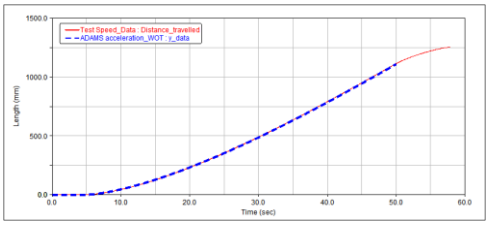

Figure 3-10: Acceleration : Distance Travelled vs. Time

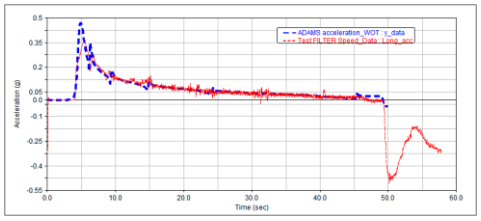

Figure 3-11: Acceleration : Longitudinal Acceleration vs. Time

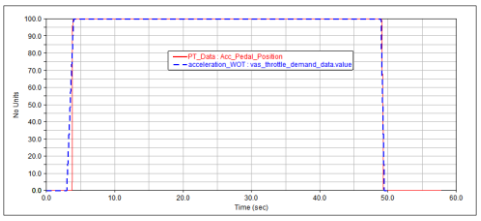

Figure 3-12: Acceleration : Throttle vs. Time

Analysis indicates that the vehicle shows the same acceleration rate as the test vehicle. The vehicle velocity and the distance travelled are the same as test. These comparisons validate the accurate modeling of the powertrain losses, aerodynamics forces and shift strategy, ultimately providing well correlated results to the acceleration response of the test vehicle.

3.3.2. Braking :

The objective of this test is to determine the braking performance of the vehicle under specified speed and maximum effort braking condition on paved road surface with friction co-efficient of 0.93. Simulation used applicable portions of TOP 2-2-602 as a general guide for conducting this test same as the physical test.

In Adams™, during a braking analysis, the Driving Machine ramps the brake input from zero at a constant rate over a specified interval of time. For this analysis, the primary results of interest are the longitudinal deceleration, vehicle speed, stopping distance.

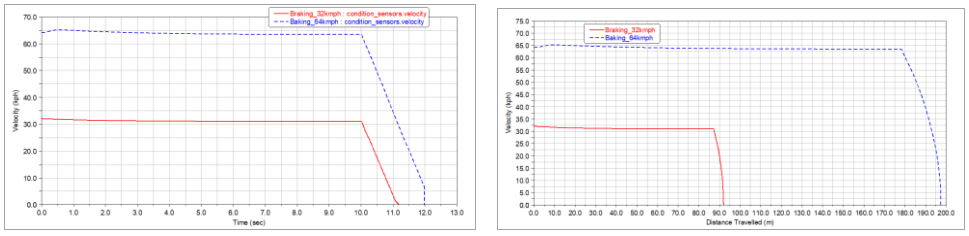

Figure 3-13: Braking : Vehicle Speed vs. Time, Distance Travelled vs. Time

After processing, the stopping distance from the distance travelled plots are tabulated and compared with the test. The results show close agreement between the simulation and test stopping distances.

Table 3-3: Stopping Distance

Braking Stopping Distance		
Speed (Kph)	Test (m)	Simulation (m)
32.2	7	6.13
64.4	27.4	25

3.4.Lateral Dynamics:

3.4.1. Double Lane Change:

For this event, both the physical test and model validation were performed according to the specifications in AVTP 03-160W. This standard specifies the track layout based upon the vehicle dimensions.

Although the event specification calls for determining a maximum course speed, the event was performed at a fixed speed of 30 mph (48.3 kph) on paved road surface (mu=0.93) for validation purposes. The measured steering wheel angle from the test was used as an open-loop input to the Adams™ model and the vehicle response was compared to the measured response.

For this analysis, the purpose is to validate lateral vehicle response, so the primary results of interest are the lateral acceleration, vehicle speed and roll angle. Below, plots of these results are compared with test, indicating very good correlation.

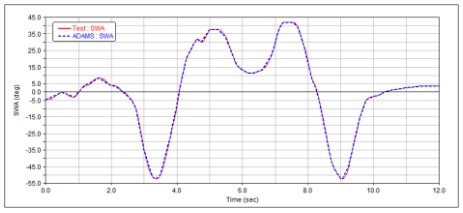

Figure 3-14: DLC : Steering wheel Angle vs. Time

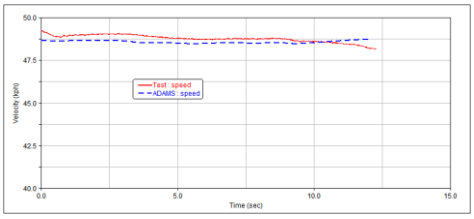

Figure 3-15: DLC : Vehicle Speed vs. Time

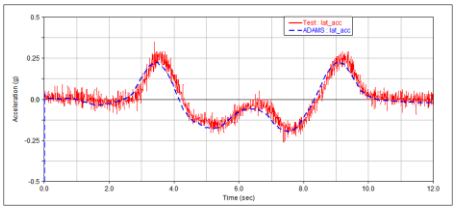

Figure 3-16: DLC : Lateral acceleration vs. Time

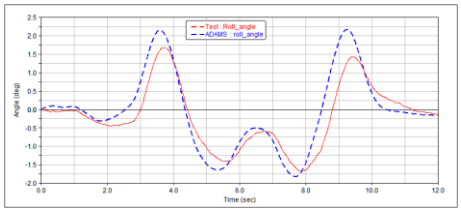

Figure 3-17: DLC : Roll Angle vs. Time

Note that additional double lane change analyses investigating the maximum attainable vehicle speed on this course via closed loop steering control were performed. These results are discussed in section 4.2.1.

3.5.Ride Quality

3.5.1. Half Rounds:

The objective of the test is to evaluate the vehicle vertical response while negotiating half-round obstacles and to determine the speed of the vehicle that generates 2.5 g peak acceleration when measured at the driver's seat base. The validation test was conducted on a 254 mm (10 inch) half round. The vehicle is driven over the half-round obstacle at multiple constant speeds with the goal of determining the speed of

vehicle that generates 2.5g peak acceleration. A speed increment of approximately 3 km/hr (2 mph) was used in this case.

For this analysis, the primary results of interest are the seat base vertical acceleration and vehicle speed. Plots of the results compared with test are shown below. This test shows good correlation with test.

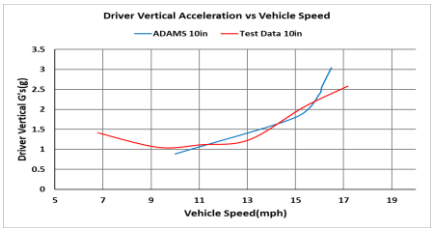

Figure 3-18: Half Rounds : Seat Base Vertical Acceleration vs. Vehicle Speed

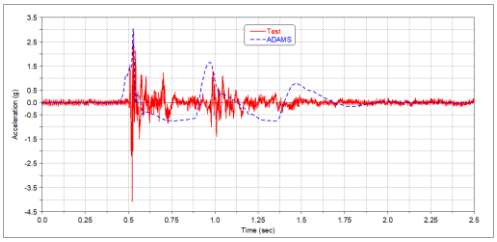

Figure 3-19: Half Rounds : Seat Base Vertical Acceleration vs. Time

The predicted vehicle speed that generates a 2.5 g peak acceleration at the seat when the vehicle strikes the 10-inch (254 mm) halfround is close to test speed results, as well as the general acceleration versus speed trend. The test acceleration results show significant high-frequency content, indicating excitation of the body compliance in this event. Additional simulation fidelity for this event could be obtained by incorporating a flexible chassis and a high-fidelity tire model. Note that further analyses on half rounds of 4, 8 and 12" were also performed, and these results are discussed later in section 4.2.3

3.5.2. RMS Course:

The objective of the test is to evaluate the system response while traversing RMS courses and determine the speeds of the vehicle that generate 6W absorbed power at the driver's seat base. In general, the roughness of a cross-country path or unpaved road can be characterized by the root-mean-square of the surface amplitude. Often, for vehicle testing and evaluation purposes, road surfaces corresponding to predetermined RMS characteristics are created at the test facility. The vehicle is driven over each road at multiple constant speeds, and following each run the absorbed power is calculated to check if the 6W power is reached for the combination of vehicle speed and the course profile. A speed increment of approximately 1 mph is used when attempting to determine the 6W vehicle speed.

For model validation, only the 2" RMS course constructed at KRC was used. For this analysis, the

primary results of interest are the seat-base vertical acceleration, resultant absorbed power and vehicle speed. Below plots of the results comparison with test. This test shows good correlation with test.

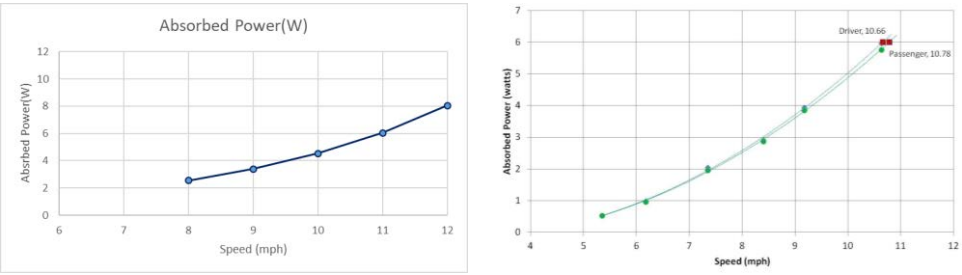

Figure 3-20: RMS : Seat Base Vertical Acceleration vs. Vehicle Speed

Additional vehicle performance predictions on other RMS courses are presented in subsequent report section 4.3.2

3.6.Traction Behavior:

3.6.1. Drawbar Pull:

The objective of the test is to determine the maximum tractive effort of the vehicle and response of the system on multiple soil surfaces. During this test the vehicle is driven with constant wheel velocity, and its forward motion is resisted by an external force applied at its drawbar (a towing hitch).

Vehicle model validation tests were conducted on both coarse-grained sand and fine-grained soil surfaces. Fine grain soil surface tests were conducted under both dry and wet conditions. Standard In-situ soil tests were carried out on each soil type and the soil characteristics were fitted for the Bekker-Wong simple terramechanics parameters [1]. These parameters were used in simulations to validate the vehicles traction behavior on the specified soil types.

The drawbar pull, travel reduction (slip), and rolling resistance are the main criteria to describe the traction behavior of off road vehicles. Drawbar pull is the force available at the drawbar, and is equal to the difference between the driving force developed by the wheels and the total motion resistance acting on the vehicle. Often, this is normalized using the vehicle vertical supporting force to calculate an effective tractive effort, which is then plotted versus percent tire slip.

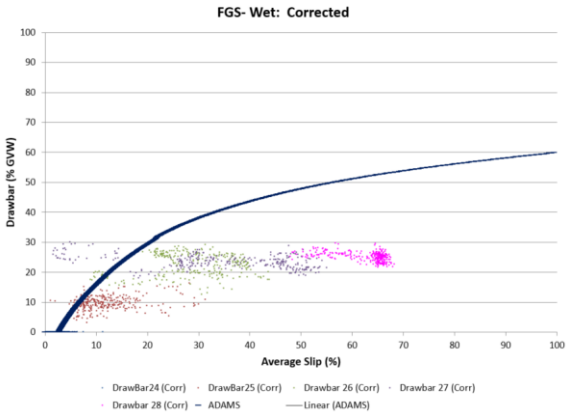

Figure 3-21: Drawbar : Tractive Co-efficient vs. Average longitudinal Tire Slip – Fine grain Sand, Wet

This study serves as the baseline study for the traction behavior of the vehicle on various soil conditions which are used by the mobility traverse events. While the traction curve shown above does not compare particularly well to the test results (clouds of points), it was found to agree more closely with other software vendors and theoretical prediction from the Bekker-Wong formulas. In this case, it appears that the simplified terramechanics theory and/or experimental soil property results are not especially accurate. Some potential sources of error include the scale of the vehicle test versus the soil tests, soil transport effects, and tire traction details. Simplified terramechanics traction limit predictions for other soil types are presented in Section 5.1.1

References

[1] Wong, J.Y. 2008. Theory of Ground Vehicles. *John Wiley & Sons, Inc.,* USA, Fourth edition.

Chapter 4 – Non-Deformable Terrain Vehicle Performance Predictions

Eric Pesheck and Venkatesan Jeganathan
MSC Software Corporation, United States

4.1. Introduction

It is required that before undertaking a mission involving a ground vehicle in rough terrain conditions, a trustworthy and thorough understanding of the mobility capabilities of such a vehicle is needed. This can be achieved by means of virtual simulation involving both terrain properties and vehicle performance limits. Virtual simulation requires a validated model reproducing the physical test results. Using a non-validated model prompts misleading results on the mobility predictions. Hence, it is critical to have a validated model. Once the model is validated, either through test comparison (as discussed in Chapter 3), or my leveraging previously validated and trusted methods, it may be used for more predictive investigations. In this report, these predictive investigations have been separated into deformable and non-deformable categories. The non-deformable tests are described here in Chapter 4, while the deformable results are covered in Chapter 5.

The tests below were conducted to evaluate the performance and mobility of the FED-Alpha vehicle on rigid terrain. Table 4.1. Presents a summary of the tests and corresponding objectives. These tests were conducted with the virtual models and subsequently compared with test results.

Table 4.1: FED- Alpha Rigid Terrain "Automotive" performance tests

Automotive Performance	
NATO Lane Change	To determine the dynamic stability of the vehicle during emergency lane change maneuvering on both paved and gravel surfaces
Gradeability and Side Slope	a. To determine the operating characteristics of the test item on the longitudinal grades and side slopes
	b. To evaluate the test item's service and parking brakes on the longitudinal grades and side slopes
Ride Quality	
Half Rounds	To evaluate the system response while negotiating half-rounds and determine the speed of the vehicle that generates 2.5 g peak acceleration at the driver's seat
RMS Courses	To evaluate the system response while negotiating RMS courses and determine the speeds of the vehicle that generate 6W absorbed power at the driver's seat
Standard Obstacles	
V-ditch	To determine if the test item can negotiate V-ditch obstacles
Vertical Step	To determine if the test item can negotiate vertical obstacles

The following sections of this chapter detail the test methodologies and results of the next generation NATO Reference Mobility Model (NG-NRMM) analysis effort within the Adams™ Car environment for the

events listed above.

4.2.Automotive Performance

4.2.1. Double Lane Change:

The FED-Alpha virtual Adams™ Model was simulated as per the specifications in AVTP 03-160W. This standard specifies the track layout based upon the vehicle dimensions. The lane change event has been simulated on both a paved surface (mu=0.93) and gravel (mu=0.37) to find the max speed that the vehicle could negotiate the course without crossing the course boundary.

The lane change course reflecting the AVTP 03-160W standard, given for the vehicle length and width is built for the event simulation. A specialized Adams™ template has been developed for this event, including graphics for the cones and lane boundaries, as well as instrumentation for easily determining if an analysis has successfully stayed within the lane boundaries. For this event, the vehicle position is monitored by coordinate systems affixed to each corner of the vehicle, and these positions can easily be evaluated relative to the course boundary.

The course boundaries are specified to depend on the vehicle width, as well as the vehicle length. For this vehicle, the measured dimensions are: Length: 183 in (4648.2 mm). Width: 89.8 in (2280.92 mm).

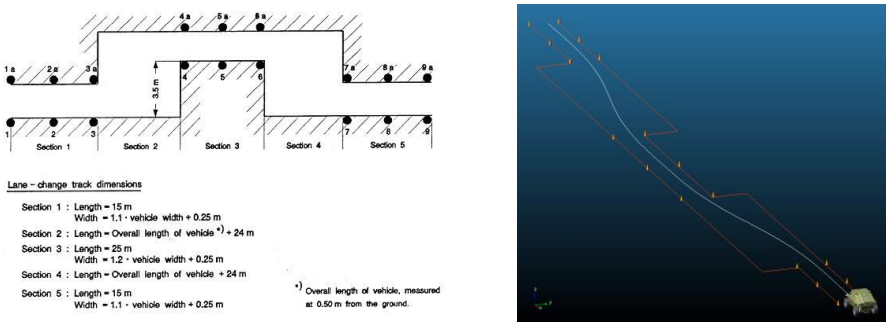

Figure 4-1: AVTP 03-160W standard course and Target Path

The vehicle, lane change course and target path are shown above.

Simulation of the double lane change event is typically troublesome, due to the complex vehicle control scenario coupled with the goal of maximizing speed without leaving the course or losing wheel contact. The process used here was iterative:

1. Tune control gains and target path coordinates to achieve acceptable baseline performance
2. Run the model with increasing speed until failure occurs.
3. Tune path or gains if appropriate
4. Further increase speed if possible until max course speed is achieved

For this analysis, the primary results of interest simply indicate the position of the vehicle relative to the course. This involves generating output for the lateral and longitudinal positions of the four vehicle corners. Having these output channels then also enables the calculation of a "margin" channel that reports the minimum distance outboard from the vehicle corners to the course boundary.

Analysis indicates that the vehicle can navigate the course on the paved surfaces at maximum speed of 43.5 mph.

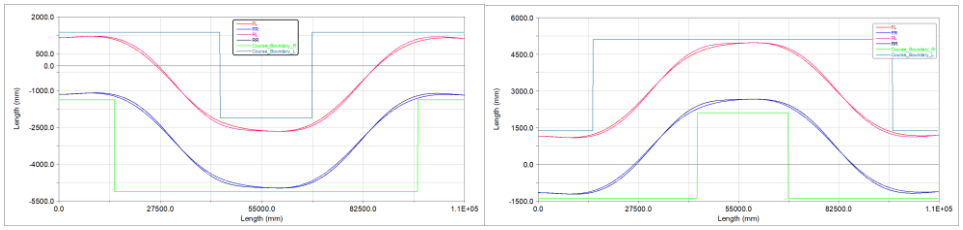

Figure 4-2: DLC : Path of vehicle corners at 43.5 mph, (left & right turn), Paved

The plot above illustrates the path taken by the four courners of the vehicle, relative to the course boundary for the paved analysis at 43.5 mph. It can be seen that the vehicle remains on the course. The plots below provide some additional clarity.

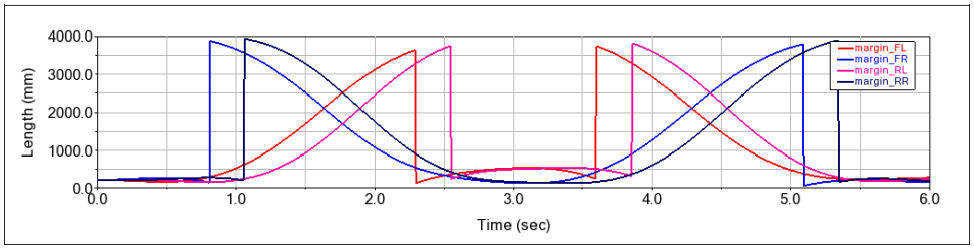

Figure 4-3: DLC : Clearance Margin to course boundary at 43.5 mph, All Corners, Paved

The plots show the instantaneous clearance margin for the individual corners (top), and the minimum of all four corners (bottom). If any portion of the curve in the bottom plot becomes negative, it indicates that the course boundary was crossed and the run would not pass. In this case, margin remains positive throughout the simulation, indicating that all corners of the vehicle remained on the course. Note that the square corners of the course boundary result in sudden jumps in the margin value as each corner in the course is cleared.

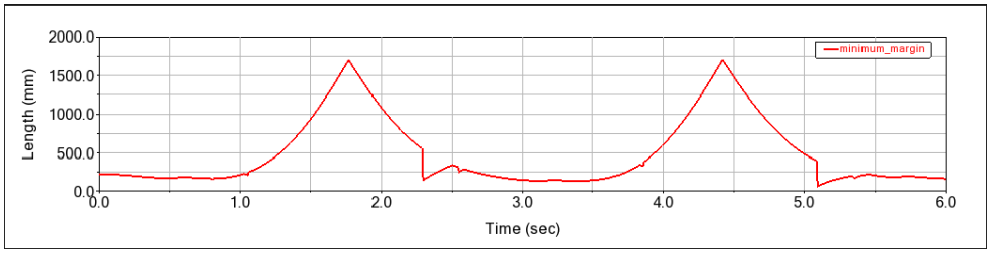

Figure 4-4: DLC : Minimum clearance margin to course boundary at 43.5 mph, Paved

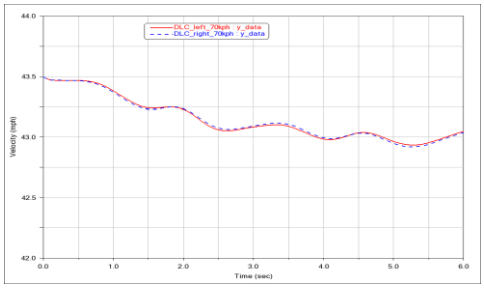

Figure 4-5: DLC : Vehicle Speed vs. Time, Paved

The plot above shows that the vehicle maintained a speed close to 43.5 mph throughout the course. Below are plots of the body roll angle for left and right turns.

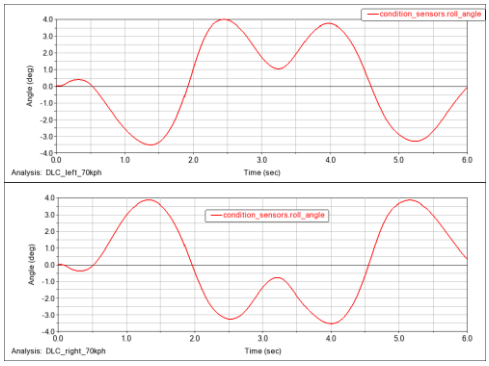

Figure 4-6: DLC : Vehicle Roll Angle vs. Time, Paved

The plots below are similar to those above, but for the gravel case. Analysis indicates that the vehicle

can navigate the course on the gravel surface at the maximum speed of 40 mph. Note that the difference between the front and rear wheel paths is more severe than that shown above for the paved case.

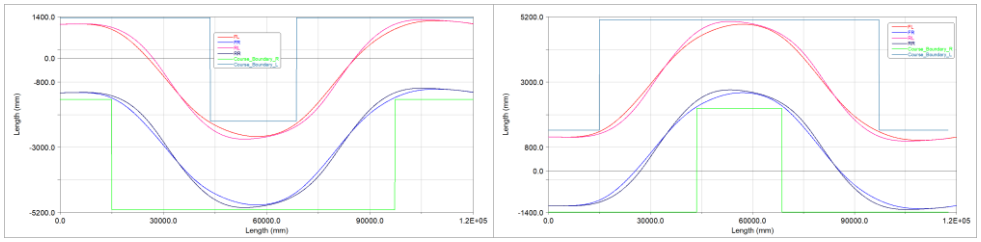

Figure 4-7: DLC : Course Top View, Paths of Vehicle Corners, Gravel

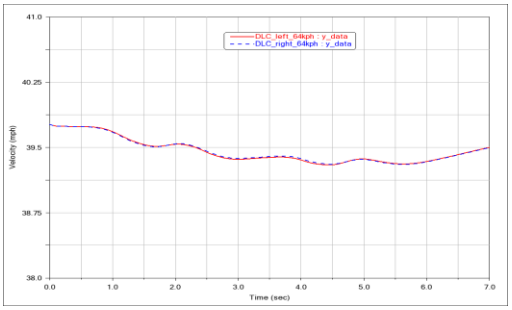

Figure 4-8: DLC : Vehicle Speed vs. Time, Gravel

The plot above shows that the vehicle maintained speed close to 40 mph throughout the course. Below, plots of the body roll angle for left and right turns are shown.

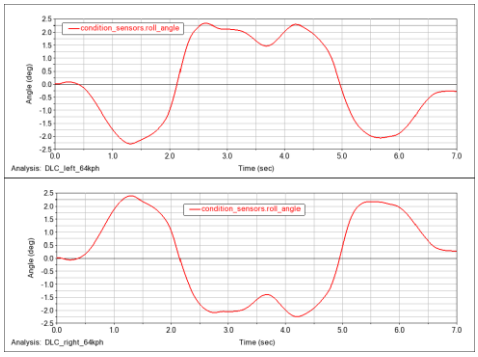

Figure 4-9: DLC : Vehicle Roll Angle vs. Time, Gravel

Based on these analysis results we observe that the vehicle is limited by traction loss due to side slip for both paved and gravel surfaces. For this event, a rigorous test of the FED vehicle capability was not performed, due to the risks involved. Hence, no comparisons to the test results can be presented, beyond what was already shown in Chapter 3. However, the results here are similar to other pre-existing vehicle performance data, as reported by Ricardo.

4.2.2. Grade Climbing:

The purpose of the event is to find the top vehicle speed for each graded slope and the maximum graded slope that the vehicle can ascend. Multiple roads were created using the Adams™ Road Builder tool, to be able to test multiple grades. Roads with grades from 30% to 100% were created, with a 5% incline between each. The grade climbing event was simulated on both a paved surface (mu=0.93) and gravel (mu=0.37) to find the max speed that the vehicle could achieve on each grade.

The Adams™ velocity controller was setup so that the vehicle would start at a low initial velocity (3.1 mph, 5 km/h), ramp the throttle to 100%, and maintain full throttle until a constant velocity is achieved by the vehicle. For grades below 55% the simulations were performed with both differential locked and unlocked conditions to find the maximum speed of the vehicle regardless of the differential settings. All higher grade runs were setup with the differential in the locked condition.

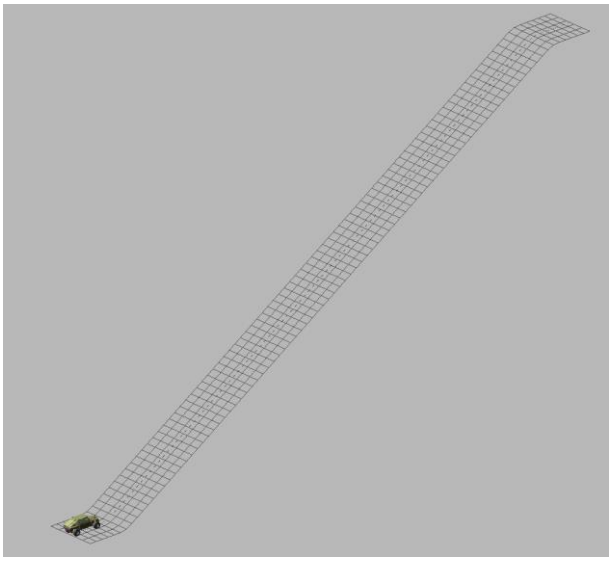

Figure 4-10: Grade Climbing Event – up-slope

The grade climb event gave the following results:

Table 4-2: Grade Climb – limiting speeds

Grade	Paved		Gravel	
	Success	Max Vehicle Speed (mph)	Success	Max Vehicle Speed (mph)
30%	Yes	13.7	Yes	13.7
35%	Yes	9.28	Yes	9.28
40%	Yes	8.98	Yes	8.98
45%	Yes	8.67	Yes	8.67
50%	Yes	8.18	Yes	8.18
55%	Yes	7.54	Yes	7.54
60%	Yes	6.89	Yes	6.89
65%	Yes	6.34	No	-
70%	Yes	5.8	No	-
75%	Yes	5.22	No	-
80%	Yes	5.19	No	-
85%	Yes	4.33	No	-
90%	No	-	No	-

The limiting factor for running the vehicle up on the slope with increased speed is the tire slip. Based on the analysis results, we observe the vehicle is limited by traction loss due to longitudinal slip for both paved and gravel surfaces. The vehicle could traverse on paved grade until up to 85% and to 60% on the gravel grade. The maximum attainable speed was 4.33mph on the 85% paved grade and 6.89mph on the 60% gravel grade. No physical data from the tests were available for comparing these performance predictions.

4.2.3. Side Slope Stability

The purpose of the side slope event is to assess the vehicle capability to negotiate around an obstacle on a side slope of 30% at low speed. The event is specified as follows:

1. 20 meter straight path.
2. Downhill obstacle avoidance around a 3 meter wide obstacle. Vehicle should recover back to the original straight line path within 30 meters (15m on either side of obstacle).

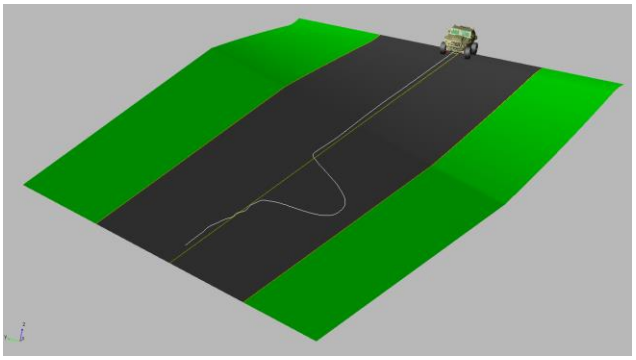

Figure 4-11: Side Slope Event

The Adams™ velocity controller was setup so that the vehicle would start at a given velocity, and try to maintain this velocity throughout the analysis. The target path has been setup so that it is straight through 40m, goes around the obstacle in 30m, and then remains straight for the final 20m. The image above shows the road surface and achieved vehicle path. The road was modelled as packed gravel, so it was treated as rigid, with a 0.47 coefficient of friction. It was observed that the vehicle could effectively follow the path at approximately 5 kph.

The following plot shows the global XY-position of the wheel centers throughout the event. Please note that the vehicle is traveling in the negative global X-direction (from right to left on the plot). The vertical spec lines indicate the bounds of the allowed 30m path deviation. The lateral limit of the obstacle, located at -90m, is at y= -4,000 mm in the plot below.

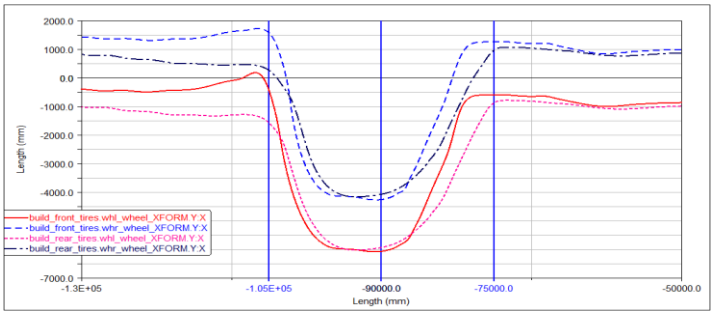

Figure 4-12: Side Slope: XY Plane, Vehicle Path, Gravel

The plot below shows the vehicle speed behavior through the event. There is some speed gain associated with turning down hill, followed by some struggle to retain and regain speed while climbing back to the original path.

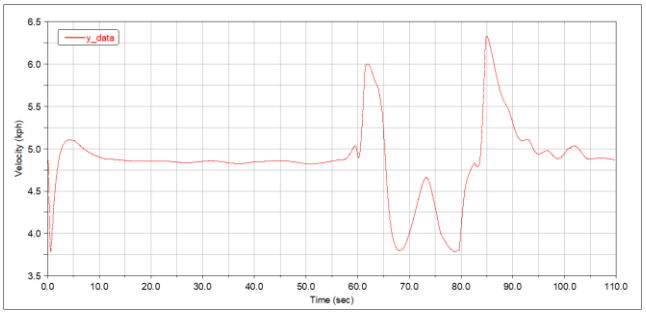

Figure 4-13: Side Slope: Vehicle Velocity, Gravel

Based on the analysis results we observe the vehicle is does not loose traction or spin out during the obstacle avoidance. No wheel lift or excessive sliding of the tires are reported. The FED-Alpha vehicle displayed similar qualitative performance and could negotiate around an obstacle on the side slope of 30% at approximately 5 kph.

4.3.Ride quality

4.3.1. Half Round Obstacle ride limiting speeds

The half round road event is intended to determine the maximum speed of the vehicle over half round obstacles of various sizes, subject to a 2.5g acceleration limit at the driver. For a given half-round size, the peak driver z-direction accelerations are recorded at a high sampling rate (1000 Hz) as the impact is simulated for progressively increasing vehicle speeds. The road is modelled as flat, except for the semi-circular half-round obstacle along the vehicle's path. For these analyses, the tire contact characteristics are significant contributors. While efforts were made to use appropriate nonlinear tire force-deflection behavior, approximations inherent to the PAC2002 tire model compromise accuracy for distinct obstacles. A more detailed tire model, such as Ftire, could be expected to significantly improve the accuracy of the tire forces for this type of analysis event.

Figure 4-14: Half-Rounds : Road setup

Limiting speed at a vertical driver acceleration of 2.5g was determined for all the half round roads (4",8",10" and 12") and compared to the test predictions.

The plot below summarizes the peak acceleration predictions, as compared to the test results. In general, the results indicate good agreement between simulation and test. The 8-inch results are one exception to this, where the test results are significantly more severe than simulation. Likely, the road/tire contact methods underpredict the tire penetration for this case. As mentioned earlier a more detailed tire model, such as Ftire, would likely address this issue.

Table 4-3: Vehicle limiting speed for 2.5g acceleration at driver seat base

2.5g accln Speed	Speed (mph)	
	Test	ADAMS
4-inch	-	-
8-inch	22	31
10-inch	17.18	16.1
12-inch	16	15.5

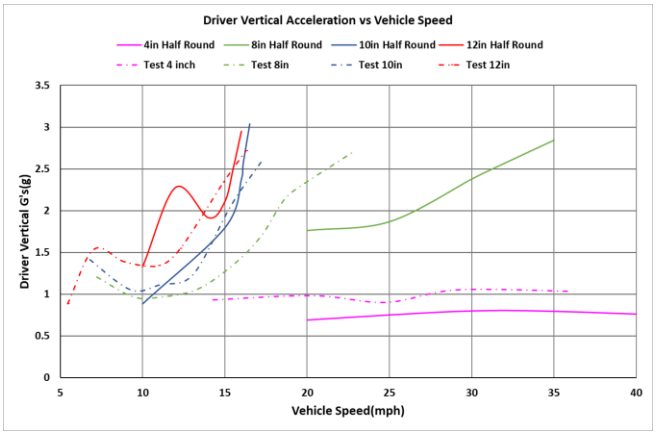

Figure 4-15: Half Rounds : Driver Z-Direction Peak Acceleration versus Vehicle Speed

The mobility of this vehicle is not significantly limited when traversing obstacles with the equivalent profile of a 4 in half-round or smaller. For obstacles above that size, traversal speeds should be limited according to the above predictions to avoid transmitting potential hazardous vibrations to the driver.

4.3.2. RMS Courses

The RMS Course event is intended to determine the maximum speed at which the vehicle can traverse a specified RMS road amplitude without exceeding the 6W maximum driver absorbed power threshold. The driver z-direction acceleration is obtained from the vehicle and is then processed to compute a driver absorbed power for each vehicle speed/road combination. That absorbed power is limited to 6 Watts for occupant safety.

For this event, the vehicle was driven across 7 different symmetric and asymmetric RMS courses. On each road the vehicle was driven the entire length of the provided road profile at a constant speed. The event was repeated at incrementally increasing speeds until the 6W driver absorbed power threshold was exceeded.

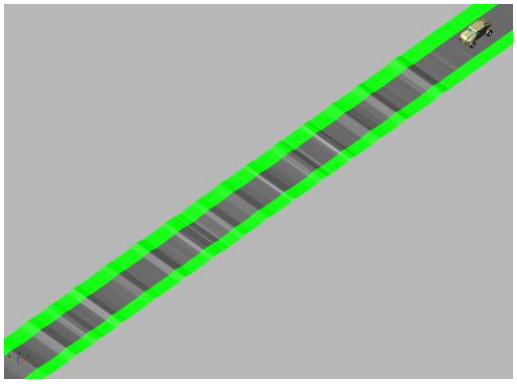

Figure 4-16: FED Alpha vehicle on 3inch RMS road

The Adams™ Car velocity controller was set to maintain a constant velocity for each analysis. For this simulation, vertical accelerations were measured at the driver's seat base location. Absorbed power calculations are carried out from the measured vertical accelerations. A sampling rate of 100 steps per second was used in MSC's power calculations. The speeds were increased after each run until the absorbed power exceeded 6W. The calculation of absorbed power is an implementation of TOP 1-1-014A CN1, which applies a frequency-weighted scaling to the square of the seta-base RMS acceleration signal.

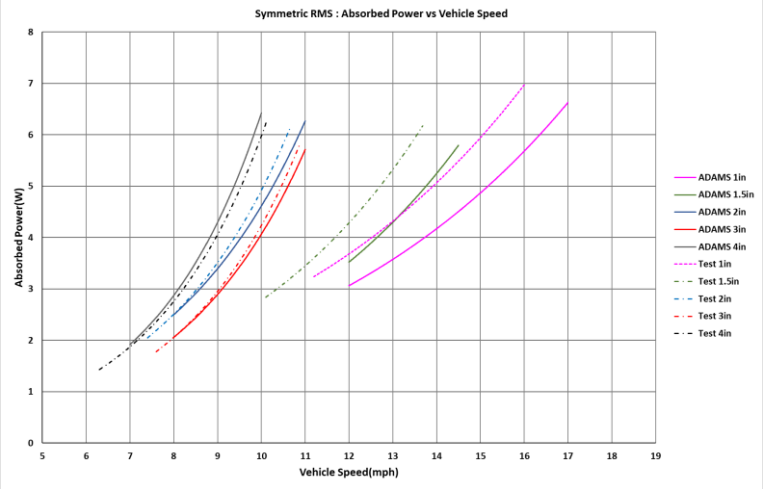

Figure 4-17: Symmetric RMS road Results

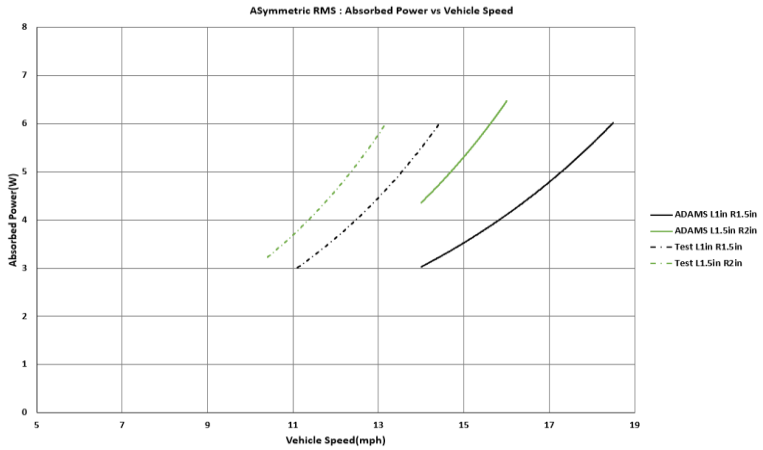

Figure 4-18: Asymmetric RMS road Results

The RMS results show remarkable agreement for most road profiles. The asymmetric profile predictions show the most room for improvement. For these, both tests include the 1.5" profile, which was the least accurate of the symmetric results. In addition, no symmetric RMS results were generated for the 1" profile, so it is difficult to develop a complete understanding of how the course symmetry contributes to the results accuracy. Lastly, the vehicle dynamic roll and torsion behavior will contribute to these results, but not the typical symmetric analyses. The decrease in fidelity relative to the symmetric road profiles could be attributed to some missing vehicle response characteristics, such as body torsional compliance.

4.4.Standard obstacles

4.4.1. Step Climb

The goal of this event is to determine the maximum traversable obstacle size. In the case of the step climb, the characteristic dimension is the step height. It is assumed that the step is approached at low speed, i.e. - less than 5.0 mph.

The modelling of the step climb was accomplished using a simple 3d-shell road file and a custom driver strategy. For this event, the vehicle control strategy was adjusted to slowly approach the step, "surge" the throttle to lift the front end, then repeat this strategy for the rear. Success for this event consisted of two criteria: 1) sufficient power and traction to climb the step, and 2) avoiding interference between the body and the road surface.

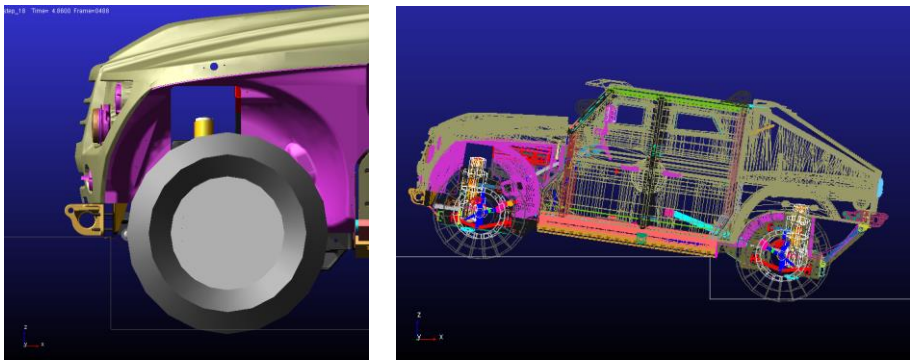

Figure 4-19: 18 inch Step climb

No special data post processing was necessary to post process the results of this event. The resulting vehicle motions were definitive in animations as to whether the vehicle succeeded in crossing the obstacle or not. Below summary of the vehicle traverse capability on the standard step obstacles.

Vertical Step	Go/No-Go	Interference
14"	Go	
18"	No-Go	Body
24"	No-Go	Body

Table 4-3: Step Climb Results

4.4.2. V-Ditch Crossing

The goal of this event is to determine the ability of the vehicle to negotiate V-ditch obstacles. The vehicle attempted to negotiate through a 35% V-ditch with a 25.5-foot span (see figure below), at an approach angle of 90 degrees to the center-line of the course (i.e. straight entry). The test was performed with the transmission set in first gear and the drive train in low range with the vehicle differentials in the locked

setting. The FED-Alpha vehicle was driven slowly into and through the V-ditch obstacle while observing for any contact or interference.

Figure 4-20: V Ditch

The V-ditch and surrounding road were modelled using a 3d-shell *road data file* format(.rdf), making direct use of the scanned triangular mesh data from the test site. The vehicle model moves with a constant velocity into the V-ditch. A brake controller was employed to maintain slow speed when the vehicle approaches the center of the ditch and a steering controller is also employed to maintain a straight path through the ditch. Throttle inputs were provided to the vehicle for climbing the rest of the V-ditch portion.

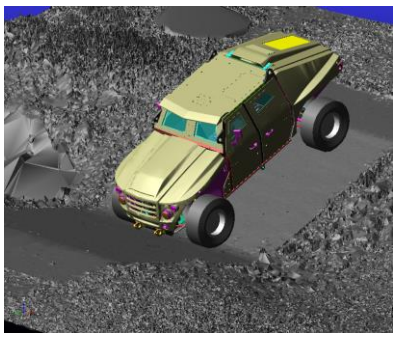

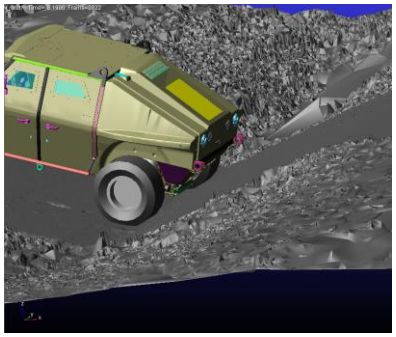

Figure 4-21: Ditch Crossing, 3D discretized road approach

The animation of the analysis results were examined closely for any contacts made by the vehicle to the ground other than tires. It is observed that the V-ditch will be successfully negotiated without interference only when the vehicle progresses very slowly through the center portion of the V-ditch.

Chapter 5 – Deformable Terrain Vehicle Performance Predictions

Eric Pesheck and Venkatesan Jeganathan
MSC Software Corporation, United States

There are a number of situations in which a vehicle may need to traverse an unprepared terrain. It may happen that the only viable means of reaching a desired objective is through an off-road route. In such an instance, it is desirable to have an understanding of how a vehicles design affects its performance in such an environment. Often, vehicles are specifically designed for off-road usage. This is the case for most military vehicles. In all cases it is important to be able to predict the conditions under which a vehicle may become incapacitated due to loss of traction.

Terramechanics is the study of soil properties, and the interaction of wheeled or tracked vehicles with various natural soil surfaces. The standard parameters by which vehicle performance is compared include drawbar-pull, tractive efficiency, motion resistance, and thrust. If the normal and shear stress distributions at the running gear-soil interface are known, then these parameters are completely defined.

5.1. Simple Terramechanics

Simple terramechanics models establish the appropriate parameters, properties, and behaviors of soil by determination of empirical relationships based on experimental results which can be used to predict the response of soils under various conditions. When a tire or a track traverses a terrain, soil is both compressed and sheared. A Bevameter is typically used to measure the terrains response to normal and shear stresses by the application of penetration plates and shear heads. These responses are then used to produce pressure-sinkage and shear stress-shear displacement curves. These curves are then taken as characteristic response curves for each type of terrain. Another terrain characterization device of importance (due to its widespread use) is the cone penetrometer. A penetrometer effectively applies simultaneous shear and normal stresses. A simplified version of a penetrometer can be visualized as a long rod with a right circular cone on one end. Penetrometers are pushed (at a certain rate) into the soil and the resulting force per unit cone base area, called the cone index (CI), is measured. Adams™ supports simple terramechanics through an implementation of the Bekker-Wong formulas for calculating tire forces based on soil deformation and wheel kinematics (slip, etc.)[2]. These methods can capture many fundamental characteristics of deformable terrain, but also cannot account for some important behaviors, such as material transport effects (digging and plowing), detailed tread influences, and some rate-dependent soil properties. As a part of the NG-NRMM effort, numerous soil tests were performed at the Keweenaw Research Center (KRC) to characterize soils associated with specific vehicle tests. Bekker-Wong parameters[1] corresponding to KRC's experimental soil results are shown below.

				Sinkage Plates							Shear Tests									
				Bekker-Wong Method					Wong Keq Method			Grouser Shear Ring					Rubber Ring				
Date	Test Set	Location	Soil	n	Kc (lb/in^{n+2})	Kc (kN/m^{n+2})	Kp (lb/in^{n+2})	Kp (kN/m^{n+2})	n Avg (Keq)	Keq (lb/in^{n+2})	Keq (kN/m^{n+2})	C (psi)	C (kPa)	Phi (deg)	K avg (in)	K avg (mm)	C (psi)	C (kPa)	Phi (deg)	K avg (in)	K avg (mm)
6/1/2018	Test Set 1	Variable Hill Climb	2NS Sand	0.40	50.3	38.8	14.6	444.2	0.39	33.6	973	0.18	1.23	32.3	0.94	23.81	0.006	0.04	26.6	0.25	6.44
6/1/2018	Test Set 2	Variable Hill Climb	2NS Sand	0.62	43.6	73.5	5.7	377.4	0.61	23.2	1522	0.21	1.47	31.7	0.75	19.08	0.000	0.00	26.9	0.44	11.19
6/5/2018	Test Set 9	Fine grain soil pit (dry)	Fine Grain Pit	1.49	-151.8	-6355.1	93.8	154544.8	1.55	48.2	99571	0.15	1.05	37.4	0.95	24.16	0.000	0.00	28.6	0.24	5.97
6/5/2018	Test Set 10	Fine grain soil pit (dry)	Fine Grain Pit	1.82	420.9	58125.4	-106.8	-580375.0	1.92	67.4	536569	0.21	1.46	35.9	0.54	13.72	0.000	0.00	29.0	0.36	9.22
6/5/2018	Test Set 12	Coarse Pit	Coarse Pit	0.46	34.6	32.5	25.3	931.8	0.55	32.7	1686	0.23	1.56	30.4	0.73	18.60	0.046	0.32	26.4	0.35	8.88
6/5/2018	Test Set 13	Coarse Pit	Coarse Pit	0.63	27.5	47.8	21.0	1437.8	0.74	26.1	2765	0.19	1.34	31.8	0.85	21.51	0.009	0.06	26.8	0.45	11.52
6/5/2018	Test Set 14	Coarse Pit	Coarse Pit	0.81	41.9	141.7	6.7	892.3	0.87	19.7	3367	0.16	1.13	31.9	0.97	24.56	0.004	0.03	26.8	0.32	8.02
6/5/2018	Test Set 17	Fine grain soil pit (wet)	Fine Grain Pit	3.57	-0.8	-73082.5	0.5	1714497.3	4.39	0.1	8236397	0.44	3.06	37.3	1.08	27.53	0.067	0.46	28.7	0.26	6.53
6/5/2018	Test Set 18	Fine grain soil pit (wet)	Fine Grain Pit	2.97	1.0	10056.3	-0.2	-81614.6	3.68	0.1	520371	0.61	4.21	33.0	1.29	32.69	0.057	0.40	28.9	0.28	7.16

Figure 5-1: Bekker-Wong parameters identified for select KRC soil tests

5.1.1. Drawbar Pull

Drawbar Pull tests are performed in order to characterize the available tractive force of a given vehicle on a specific soil. They are considered a key indicator of vehicle capability on deformable terrain. For this study, tests were conducted on both coarse-grained sand and fine-grained soil surfaces. In addition, the fine grain soil surfaces were tested under both wet and dry moisture conditions. The tractive effort curve of the FED-Alpha vehicle was generated on both coarse-grained sand and fine-grained soil surfaces using a time-domain vehicle simulation where the vehicle attempted to maintain a steady speed while subjected to an increasing drag load. Initial simplified terramechanics results were generated on fine-grain wet soil as a part of the model validation effort, and these were presented in Chapter 3. Additional results for more soil types are summarized below.

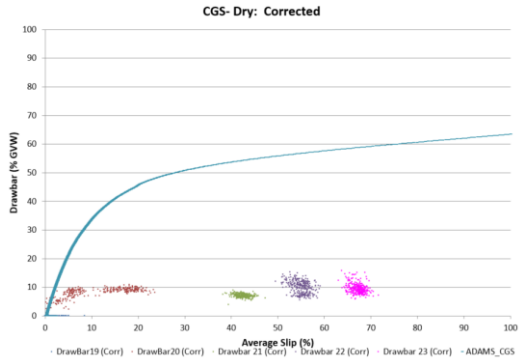

Figure 5-2: Tractive Co-efficient vs. Average longitudinal Tire Slip – Coarse grain Sand, Dry

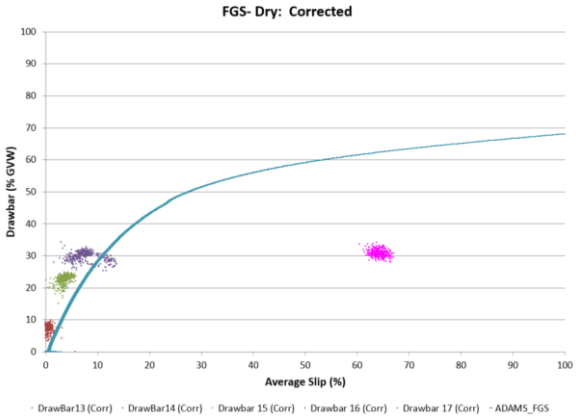

Figure 5-3: Tractive Co-efficient vs. Average longitudinal Tire Slip – Fine grain Sand, Dry

Note that the Adams™ results are reasonably predictive for slip ratios below 15% on the fine grain dry soil, but tend to overestimate the available traction at high slip ratios. On coarse grain sand, the predictions significantly overestimate the available traction. Upon examination, the calculated behavior was generally consistent with Bekker-Wong theory (and broadly similar to other simplified terramechanics vendor results.) This implies that the primary issue with predictions on coarse grain sand is that the soil is either not behaving in a manner that is well represented by the Bekker-Wong formulation, or the soil characteristics are not consistent between the vehicle and soil testing scenarios.

5.1.2. Variable Sand Climb:

An additional assessment of the vehicle's performance was conducted using an existing variable-grade sand slope at KRC. The slope steadily increases grade from 0% (initially flat), up to about 30% at the crest of the slope. As with the other soils, the Bekker-Wong parameters for this soil were determined through Bevameter testing in the field. Within Adams™, a 3d-shell road file was created using triangle mesh data generated through a scan of the terrain. The figure below illustrates the vehicle on the terrain.

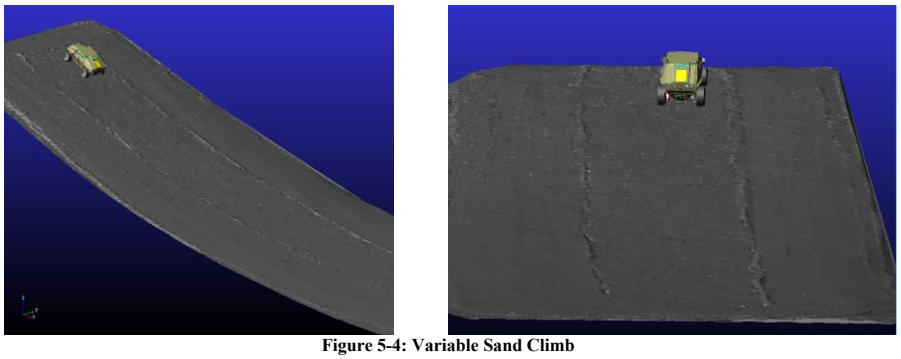

Figure 5-4: Variable Sand Climb

As shown, the Adams™ simulation predicts that the vehicle can climb the slope. In the testing, the vehicle could not progress beyond about the 13% grade point. As with the drawbar pull, it appears that the simulation results are consistent with the Bekker-Wong theory and the calculated parameters. Hence, the poor model prediction is likely due to either poor agreement between the soil and Bekker-Wong assumptions, or flaws in the testing strategy leading to inaccurate Bekker-Wong parameters.

In addition to the results discussed above, simplified terramechanics methods were employed for analysis of some simulations within the Mobility Traverse. These results are discussed later, in Chapter 6.

5.2. Complex Terramechanics (Discrete Element Method-DEM)

In contrast with the analytical formulations of bulk properties used by simplified terramechanics, it is possible to implement methods where these bulk properties emerge from particle interactions. For these cases, in which the granular behavior of soil is to be accurately modelled, the approach is referred to as discrete element method, or DEM. DEM was developed to simulate the dynamic behavior of granular material in applications such as excavation, mining or granular flow. In DEM, the material is represented by a collection of interacting particles with simple shapes (typically based on circles and spheres). The contact

properties acting between the particles are represented using a variety of spring/damper/friction formulations, allowing the representation of a wide variety of aggregate material properties. These model parameters can be difficult to obtain by direct physical measurement. Indirect methods of parameter determination are often necessary. Among them, the trial-and error approach has been used successfully and the method of dimensional analysis combined with biaxial test simulation can obtain best-fit parameters for the DEM model.[3]

There are numerous applications where it is important to understand system behavior that accounts for coupling between the MBD domain and other time-domain solvers. Recently, MSC has implemented a more formal architecture to systematically support co-simulation with specific applications. The Adams™ Co-Simulation Interface (ACSI) currently supports co-simulations between Adams™ and either EDEM (From DEM Solutions) or the MSC Marc nonlinear FEA package. The typical simulation process workflow is shown below.

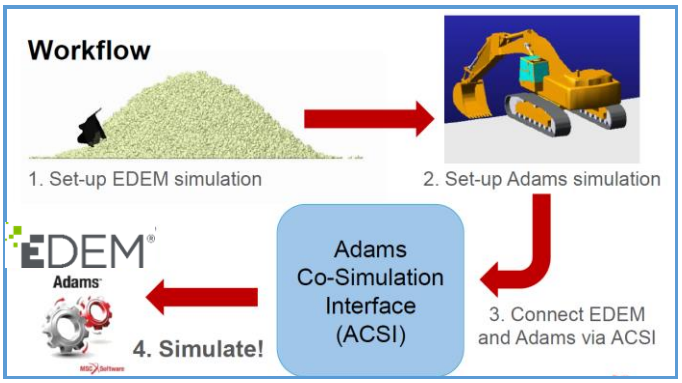

Figure 5-5: EDEM Simulation Workflow

This workflow is generalized to allow generic communication between Adams™ and EDEM, and is not tailored specifically to soil or terrain applications. At a conceptual level, potential EDEM contact is defined for designated parts. The displacement of these parts is determined by Adams™ and provided to EDEM. EDEM then determines the resultant reaction forces, which are passed back to Adams™. The communication interval between the solvers must remain small enough to ensure that the dynamic solution remains stable as these displacements and forces are exchanged.

For the NG-NRMM simulation effort, MSC's ability to investigate different Complex Terramechanics scenarios via EDEM was limited by both resource funding and program schedule. Hence, the work was limited to a single soil (fine grain wet, or FGW), and the vehicle events performed on this soil.

5.2.1. DEM Material Calibration

Often it is not practical to use a DEM model where the particle sizes are consistent with the physical material. While this may be practical for crushed rock, it is rarely the case for finer sands or soils, where a typical vehicle footprint might require 10 billion particles or more. In addition to the issues inherent to scaling up the particle size, it is rarely possible to directly measure the particle interaction in ways that can be

meaningfully applied within DEM. Hence, it is typically necessary to calibrate the DEM material properties to align with some sort of bulk property measurements of the soil.[4]

For this project, the soil calibration process is depicted below.

Figure 5-6: Calibration Process

Calibration Steps:

1. Identification of suitable soil tests: Select physical tests that can be re-created within EDEM
2. Virtual DEM Soil Test Setup: Estimate initial soil properties as a starting point
3. Material Shape & Size: Select particle size based on final application
4. Pressure - Sinkage Calibration: Iterate on select properties to improve pressure-sinkage behavior
5. Shear strength calibration: Iterate on select properties to improve shear behavior
6. Calibrated Material Bed: Prepare material bed for Adams™ vehicle co-simulation event

Step 1: Identification of Suitable Soil Tests

Identify the tests that will characterize the bulk density, angle of internal friction, stress-strain behavior of model. The poured angle of repose test, or geotechnical ASTM standard tests (tri-axial, shear, Bevameter, cone penetrometer) are typically good candidates. The Bevameter test with compressibility and shear results were identified for calibration in this case. (Specifically, KRC Test case 36 on Fine Grain Wet sand)

Step 2: Virtual DEM Soil Test Setup

A simple representative EDEM model of the experimental test is created. The virtual tests are specifically designed to capture the pressure-sinkage and shear behavior of the EDEM soil representation. A nominal soil property from the existing EDEM example soils may be used for initial parameter estimates.

Step 3: Material Shape & Size

It is computationally prohibitive to match equivalent clay, silt and sand size fractions. The size of the particles is subject to computational capability – either associated with the calibration test or the subsequent use case. In this case, for the fine grain wet soil, 18.4mm spheres were used to create approximately 50mm particles based on the full-vehicle analysis computation scale.

Step 4: Pressure - Sinkage Calibration

For the pressure–sinkage tests, circular plates of 4” diameter were used, along with data from test set 36. The sinkage values from test were used as displacement inputs to the DEM model and the resulting reaction forces from the DEM model were compared to the test results. Cone penetrator test data could not be used as the particle size was too large, relative to the cone used for testing.

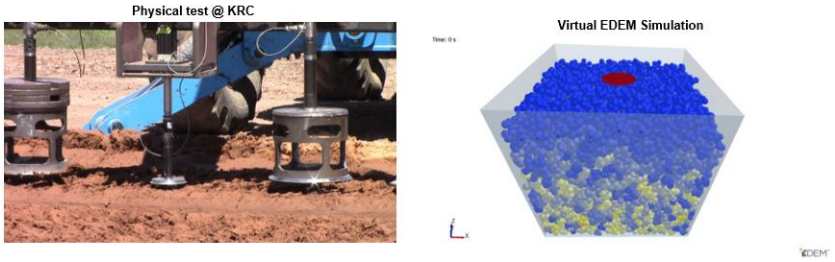

Figure 5-7: EDEM Calibration– Pressure-Sinkage test

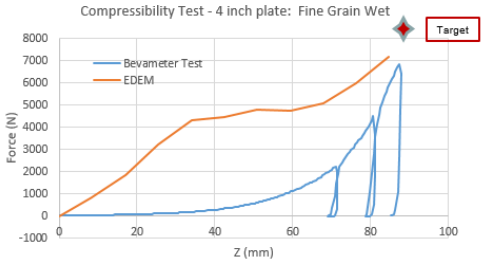

Figure 5-8: Pressure vs. Sinkage

At this stage in the NG-NRMM project, the analysis emphasis was primarily on demonstrating analysis process and capability. Soil property tuning was performed with a goal of roughly achieving appropriate behavior, especially in the neighborhood of typical wheel loads, as indicated by the "target" label above.

Step 5: Shear Strength Calibration

For the shear tests, a steel grouser with 13.3" diameter was used. Data from Test set 36 was used for calibration. Sinkage values and grouser rotation angle from test were used as inputs to the DEM model. Reaction torque from the DEM model were compared to torque values from test.

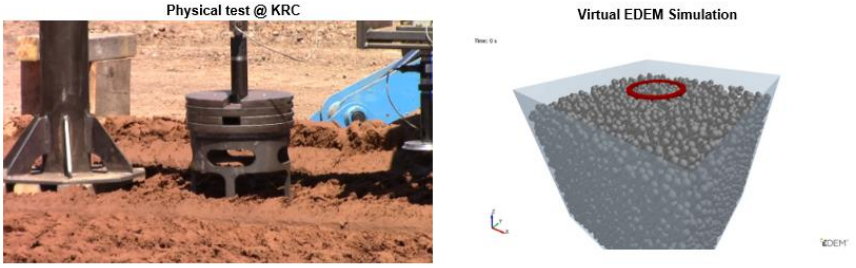

Figure 5-9: EDEM Calibration– shear strength test

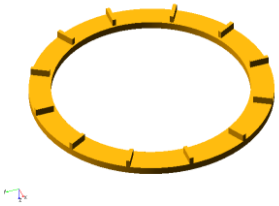

Figure 5-10: 34 cm Grouser – Shear Test

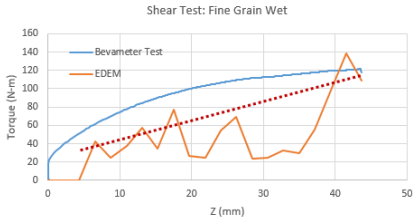

Figure 5-11: Torque vs. Sinkage

As with the pressure-sinkage relationship above, this test was undertaken with the goal of illustrating the process, and obtaining roughly appropriate soil characteristics. The shear behavior obtained indicates a trend consistent with the test behavior.

As a result of the compression and shear calibration process shown above, the final EDEM soil used the following particle properties:

- ν-Poisson's ratio 0.25
- G-Shear modulus 1.5E+8 Pa
- μs-Coefficient of static friction 0.5
- μr-Coefficient of rolling friction 0.2
- e-Coefficient of restitution 0.7

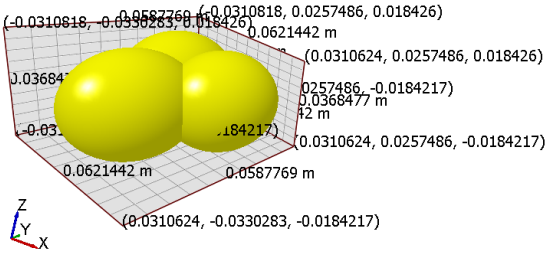

GEMM_particle_3171 Spheres

Edit Contact Radius

	Name	Position X (m)	Position Y (m)	Position Z (m)	Physical Radius (m)
1	Sphere 0	4.77782e-05	-0.0146283	2.60074e-05	0.0184
2	Sphere 1	0.0126624	0.00734862	-3.11838e-06	0.0184
3	Sphere 2	-0.0126818	0.0072871	-2.16982e-05	0.0184

Figure 5-12: EDEM Particle size

The above image shows the co-joined spheres as single particle. Also the table provides the radius and position of the individual spheres to form a particle of approximately 50mm radius. These investigations were performed using EDEM version 2018

Several challenges complicate the soil property characterization for this case:

- **Mismatch between test scale and vehicle scale**. The vehicle scale dictates the practical particle size, due to computational limitations. As a result, the particles end up quite large relative to the test scale.

- **Large particles relative to test add noise to simulation.** The size of the particles result in many discrete contact events as the calibration tests progress, resulting in significant test sensitivity to particular soil bed particle arrangements. In addition, the grouser teeth are quite short (10 mm) relative to the particle size, affecting the nature of the interaction between the grouser and the particles.

- **No process to maintain soil properties with changing particle size**. Ideally, smaller particles could be used for the soil calibration stage, and then these properties could be used to create an equivalent large-particle soil. However, no established process exists to support maintaining bulk properties as particle size changes.

- **Limited Time for calibration due to project schedule and funding**. Given sufficient time and funding, the obstacles above could likely be addressed with careful study and additional analyses. The noise associated with particle size could be averaged out through multiple simulations on similar soil beds, or it might be practical to do the initial calibration with much smaller particles and then use larger scale simulations to develop an equivalent large-particle soil representation.

5.2.2. Co-Simulation of DEM with MBD

EDEM was coupled with MSC Adams™ for dynamic simulations with deformable soil interaction. Coupling DEM with MBD will transfer transient loads from the geo-materials model into the full vehicle multibody model, and pass part displacements back into the DEM solver.

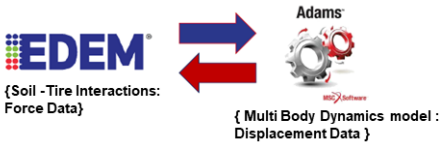

Figure 5-13: Co-simulation Adams™ with EDEM solver

Drawbar Pull test – EDEM Predictions

The drawbar test described previously in Sections 3.6 and 5.1 was repeated using an EDEM co-simulation. The plot below plot provides the resulting traction behavior predictions for wet fine-grain sand.

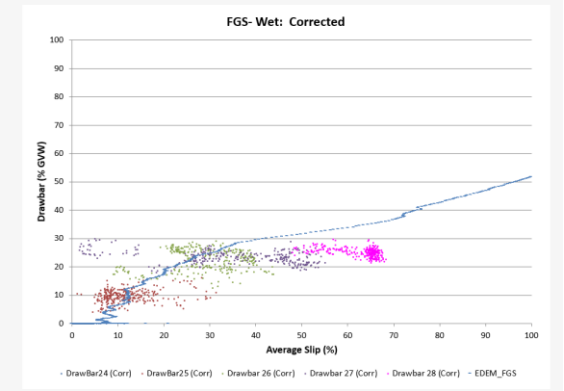

Figure 5-14: EDEM & Test Drawbar Co-efficient Vs Average Slip

The traction behavior predicted from the simulation model employing both Bekker-Wong and DEM calculation methods is compared below. Considerable difference in the behavior is observed between the two calculation methods. Though the DEM method is computationally expensive, the behavior predicted at lower tire slip angles (<40%) agrees very well with the actual physical behavior.

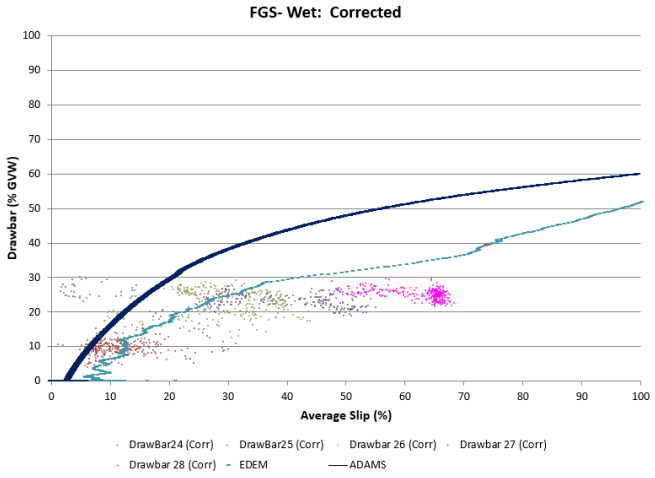

Figure 5-15: EDEM, ADAMS™ & Test Drawbar Co-efficient Vs Average Slip

5.3. Computation efforts for Terramechanics:

The table below illustrates the computational resources and the efforts for each of the EDEM analyses presented in this project, as well as comparable Adams™-only analyses where applicable. The "90-deg turn & WOT" EDEM analysis will be discussed in Chapter 6.

Soil Type	Method	Simulation Time	Wall Clock Time	Vehicle Speed	Hardware : RAM	Hardware : Cores	Hardware : Parallel Computing	OS	Test	Software
Fine Grain Wet Sand Drawbar Pull	Simple Terramechanics - Adams	22.18 s	1 min 57 s	5 mph	32 GB	8	Yes	Windows 10	Straight Line - Drawbar pull	ADAMS
Fine Grain Wet Sand Drawbar Pull	Complex Terramechanics - EDEM	8.17 s	4 hrs 8 min	5 mph					Straight Line - Drawbar pull	ADAMS & EDEM Co-simulation
Fine Grain Wet Sand Traverse Y7	Simple Terramechanics - Adams	12.42	6 min	Acceleration WOT					90 deg turn & WOT	ADAMS
Fine Grain Wet Sand Traverse Y7	Complex Terramechanics - EDEM	12.42 s	26 hrs 21 min	Acceleration WOT					90 deg turn & WOT	ADAMS & EDEM Co-simulation

Table 5-1: Terramechanics computation effort

When running vehicle analyses with EDEM, an additional "soil bed preparation" simulation was necessary in order to "pour" the soil into place and prepare it for analysis. This soil bed could be re-used for multiple simulations. In addition, a "windowing" method was used in EDEM, such that only particles within the vehicle vicinity (4.75m by 2.5m, centered on vehicle) were considered at any given moment. This significantly increases the EDEM solution efficiency.

References

[1] Wong, J.Y. 2008. Theory of Ground Vehicles. *John Wiley & Sons, Inc.,* USA, Fourth edition.

[2] MSC.Adams™ 2018 Documentation: section - Using the Soft-Soil tire model

[3] EDEM 2018 Documentation

[4] Prediction of discrete element parameters for modeling the stregthof sandy soils in wheel /soil traction applications - A dissertation Presented to the Graduate School of Clemson University by Timothy C. Reeves May 2013

Chapter 6 - Mobility Traverse Analysis

Eric Pesheck and Venkatesan Jeganathan
MSC Software Corporation, United States

The objective of the mobility traverse analyses were to assess vehicle model predictions for a continuous traverse over composite terrain representative of a typical Mission Profile (MP). The general objective was be to study the maximum speed for each traverse subject to the vehicle (acceleration and absorbed power) and terrain limits while maintaining vehicle stability and control. This assessment provides a clear contrast between predictions available through Adams™ and comparable performance predictions available through pre-existing legacy NRMM methods.

Satellite imagery and soil designations for the KRC terrain selected for FED-Alpha mobility traverse evaluation is shown below.

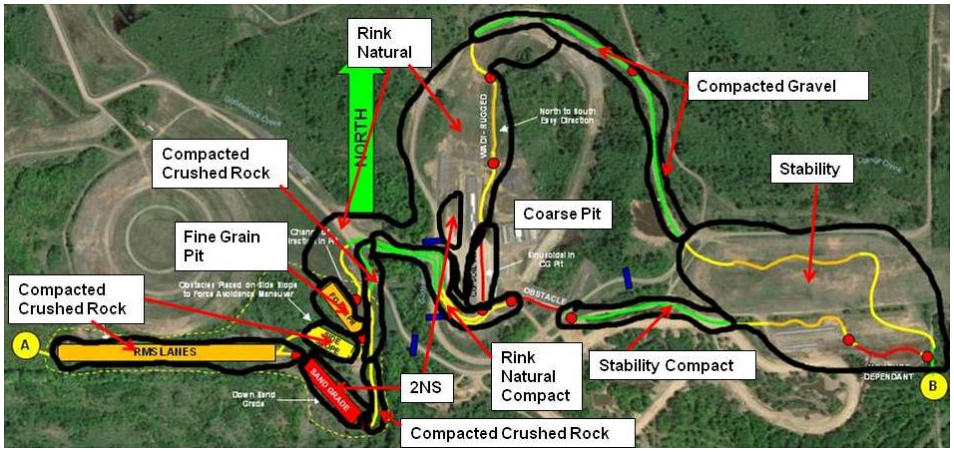

Figure 6-1: Satellite Imagery of the terrain

The terrestrial scan data for the entire terrain was made available in several formats for building virtual terrain, in support of the modeling requirements. The scan data was broken down into a number of segments to easily handle the large dataset of the triangular mesh data for the entire traverse area. The traverse event was defined to support the analysis process by breaking it into numerous discrete sections, punctuated by points where the vehicle came to a complete stop. The traverse segments were designated by a West-to-East portion (Blue) and an East-to-West (Yellow) portion, each with numbered subsections (e.g. B2 or Y7), and a total length of approx. 3.27 miles. The traverse segments and stopping points are shown in the schematic below. In addition, the black bars indicate break points between terrain scans.

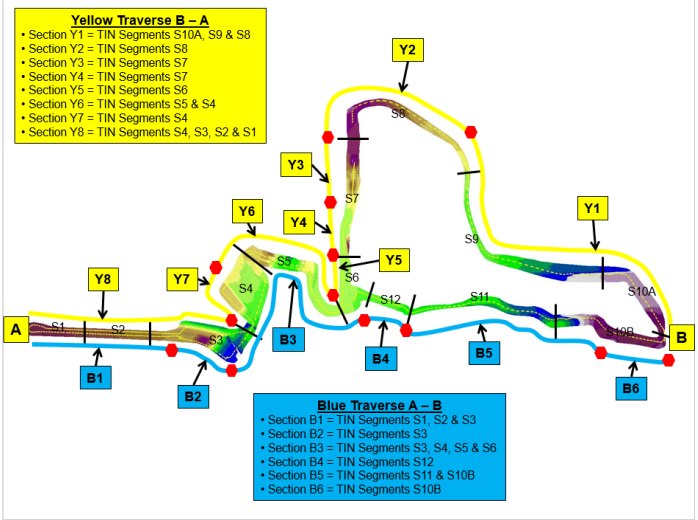

Figure 6-2: Terrain Segments

Due to the analysis effort associated with predicting maximum vehicle performance over a given segment, the traverse analyses were distributed among the participating software vendors. MSC evaluated four assigned terrain segments.

6.1. Mobility Traverse Predictions

MSC evaluated the following traverse segments for maximum obtainable end-to-end speed:

- Y1 : Transition to Secondary Road, Sinusoidal of Packed Trail, and Packed Trail , Panic Stop
- Y2 : Max Acceleration – secondary Road & Packed Trail
- Y7 :Grade climb on compact crushed rock, 90-Deg turn in FGS Wet
- B2 : Uphill on compact crushed rock, downhill on 2NS sand

The above listed traverse segments have a combination of hard and soft soil combinations which were captured accordingly. Each segment had to be sliced further into sub-segments due to either transitions between road scans or soil type. Hence, each segment of the traverse was assembled from multiple individual simulations, but the operating conditions of the vehicle, such as speed and gear conditions, were carried over carefully between analyses to accurately represent continuous vehicle behavior.

For these simulations, the target vehicle path was provided for each traverse segment and implemented within Adams™ for use by the vehicle steering controller. For each traverse simulation, the vehicle is started with an assumed speed, gear, and differential state (locked or unlocked) and driven over the terrain segment to establish a baseline safe speed. After this, the speed of the vehicle is selectively increased where possible without overturning the vehicle, losing stability, or diverging from the path. In addition, the

vertical accelerations were measured at the driver's seat base and the resultant absorbed power was monitored to confirm that the vehicle did not exceed the 6W limit throughout the segment. By doing this iterative study, the maximum speed on each terrain sub-segment was predicted. Addition of all the segment (and sub-segment) travel times would provide the time taken to travel through the full traverse route. Over each segment, the predicted speeds may be compared with the test speeds to assess the ability of virtual models to predict mobility. In the following sections, the details and results of each traverse segment are summarized.

6.1.1. Traverse Segment Y1

The traverse segment Y1 is comprised of a transition to secondary road, sinusoidal path along a packed trail, a packed gravel trail and a panic stop at the end. Simulation of this traverse segment in Adams™ was divided into four sections, shown below from right to left:

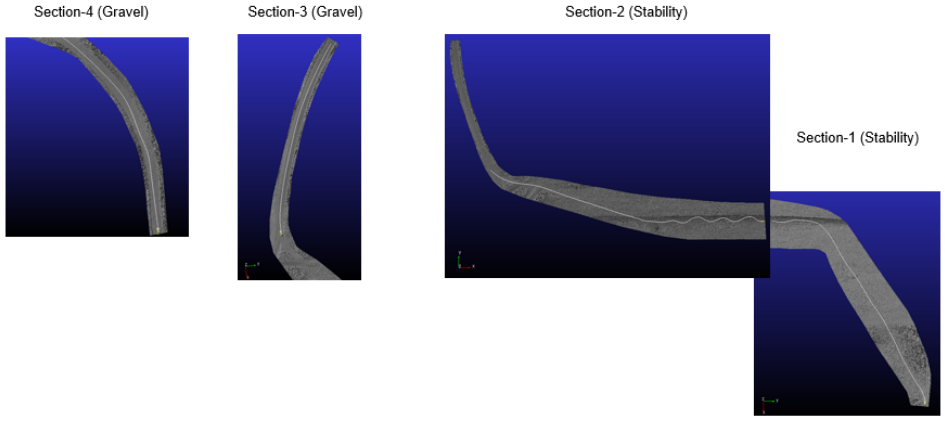

Figure 6-3: Y1 Terrain Sections

- Section-1 : Start from a stop on stability soil and apply full throttle until the turn towards the berm. Take turn and begin sinusoidal section.
- Section-2 : Continue sinusoidal path on berm, then accelerate towards gravel road and make a turn
- Section-3 : Soil type changed to gravel, apply max acceleration along gravel road
- Section-4: Continue on gravel until panic stop at max braking

Predicted vehicle velocity for the traverse segment Y1 (blue) is compared to the 3 test results (red) in the plot below.

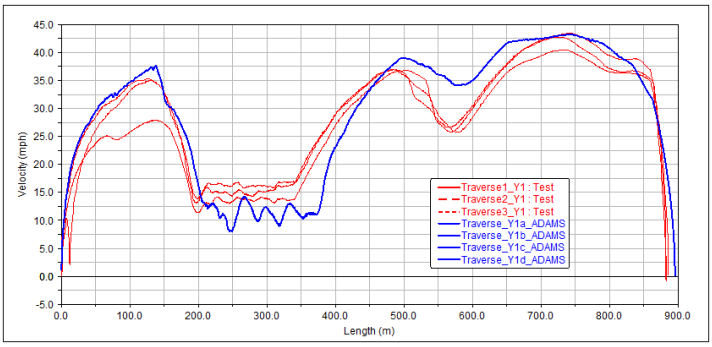

Figure 6-4: Vehicle velocity vs. Distance travelled, Traverse segment Y1

Note that the four simulation segments have been concatenated to appear as a single blue curve, with continuous speed at each transition. In general, the agreement to test is very good, although the Adams™ simulations were bit slower through the sinusoid section and a bit faster on the gravel road.

6.1.2. Traverse Segment Y2

Traverse segment Y2 starts with max acceleration along a secondary road with a transition to Rink Natural soft soil. Simulation of this traverse segment in Adams™ was divided in to two sections, as shown below, to accommodate the change in the soil types.

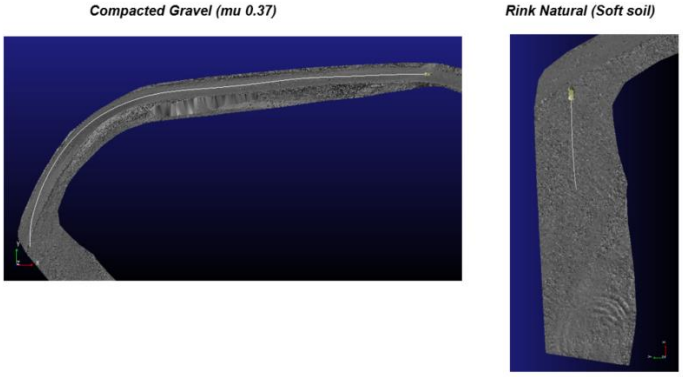

Figure 6-5: Y2 Terrain Sections

- Section-1 : Starts from a stop on Gravel and applies full throttle until the turn, slows down for the turn and subsequent transition to rink natural soil
- Section-2 : Takes over on soft soil (Rink natural sand) at a matching initial speed from section-1, then takes a turn, accelerates, and finally slows down to complete halt.

Predicted vehicle velocity for the traverse segment Y2 is compared to the test runs (red) in the plot

below.

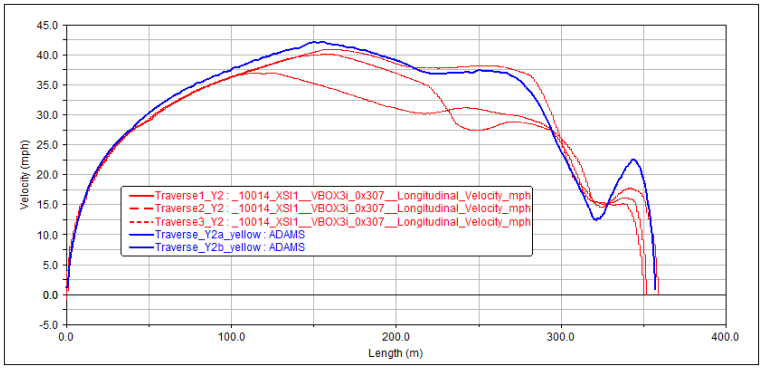

Figure 6-6: Vehicle velocity vs. Distance travelled, Traverse segment Y2

Given that both the vehicle acceleration and cornering capability was calibrated as a part of the model validation, it is not surprising that the results match quite well over most of this section. Toward the end, where soft soil traction becomes more relevant, more discrepancy is observed.

6.1.3. Traverse Segment Y7

Traverse segment Y7 starts with a short grade climb on compact crushed rock, followed by a 90-degree turn in wet fine-grain sand. Simulation of this traverse segment in Adams™ was divided in to two sections to accommodate the change in the soil types. These sections are shown below:

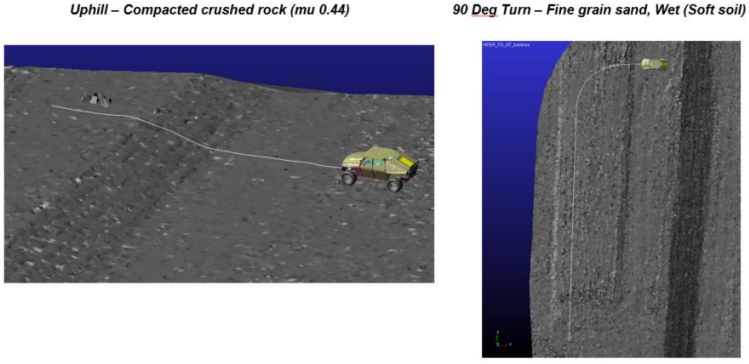

Figure 6-7: Y7 Terrain Sections

- Section-1 : Starts from a stop on flat ground and includes a short grade climb
- Section-2 : Takes over on soft soil (Fine grain sand) at a matching initial speed from the grade climb,

then takes a 90-deg turn and accelerates in the sand

Section 2 was simulated using both the Bekker-Wong simplified terramechanics model and the EDEM complex terramechanics approach. The predicted vehicle velocity for the traverse segment Y7 using the simple terramechanics approach is compared to the test in plot below.

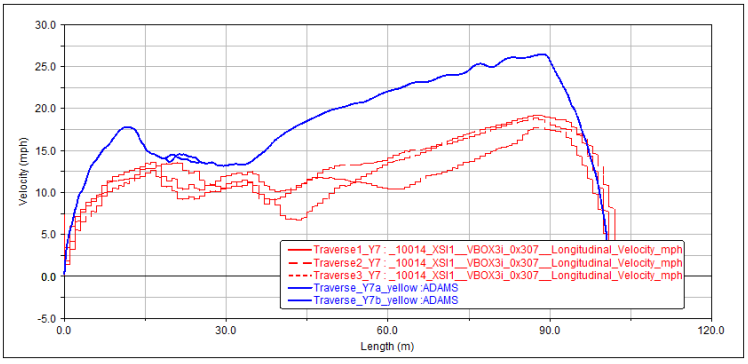

Figure 6-8: Vehicle velocity vs. Distance travelled, Traverse segment Y7 – Simplified Terramechanics

For this case, the vehicle is able to carry more speed through the 90-degree turn, relative to test. After exiting the corner with a high speed, the subsequent vehicle acceleration is roughly comparable to test.

The predicted vehicle velocity for the traverse segment Y7 using the Adams™ and EDEM co-simulation approach is compared to the test in plot below.

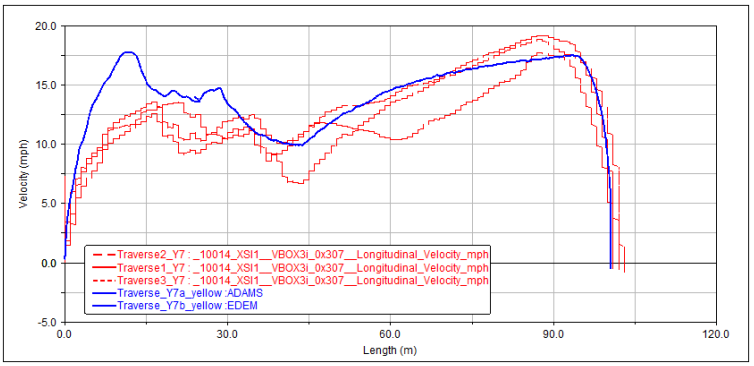

Figure 6-9: Vehicle velocity vs. Distance travelled, Traverse segment Y7, Complex Terramechanics

For these EDEM results, the initial rigid ground portion (labelled Y7a) is identical to that used above for the simplified terramechanics approach. For the second segment, more realistic speed loss is seen through

the turn, and the subsequent acceleration behavior correlates quite closely as well. This event uses the same Fine-Grain Wet sand material model described in Section 5.2 where this material model's calibration and drawbar results were reviewed. The image below illustrates the path travelled by the vehicle when modelled using discrete element modelling method. This bed contained about 339,000 discrete particles

Figure 6-10: EDEM Fine Grain Wet sand Simulation

6.1.4. Traverse Segment B2

Traverse segment B2 consisted of an uphill portion on compact crushed rock, followed by a downhill section on natural sand. Simulation of this traverse segment in Adams™ was divided in to two sections to accommodate the change of soil type.

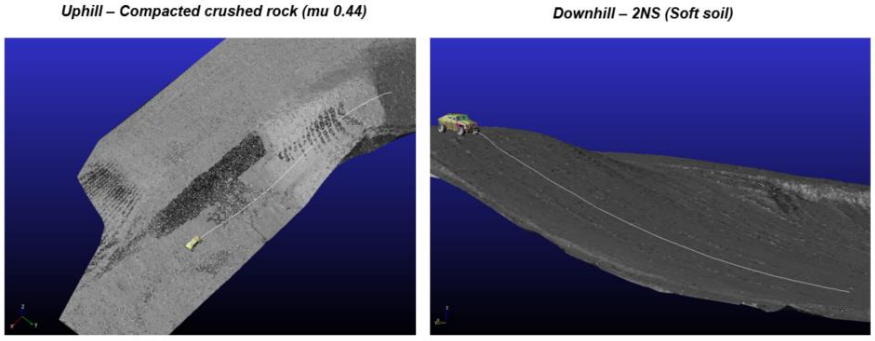

Figure 6-11: B2 Terrain Sections

- Section-1: Starts from a stop on rigid ground and includes the uphill portion
- Section-2: Takes over on soft soil (sand) at a matching initial speed from the top of the grade, descends, then comes to halt at the designated stop location.

The predicted vehicle velocity for traverse segment B2 is compared to test results in the plot below.

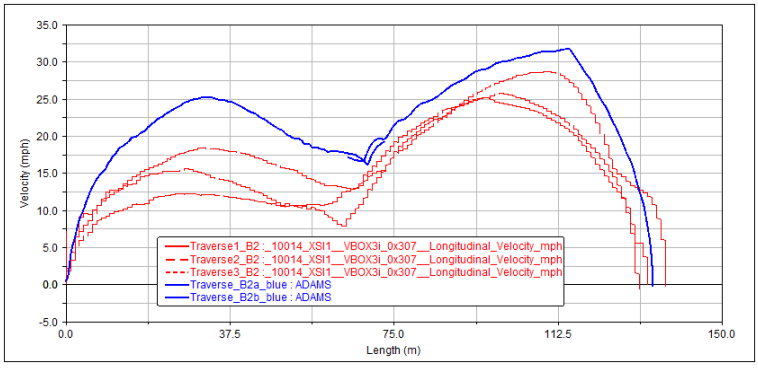

Figure 6-12: Vehicle velocity vs. Distance travelled, Traverse Segment B2

For this event, the comparison to test indicates that the model may have a bit more traction on section 1 (crushed rock), allowing the vehicle to climb at higher speed. The speed over the crest of the hill was restricted in order to maintain vehicle controllability and avoid "launching" the vehicle. Behavior through section 2, on the sand, appeared quite accurate.

6.1. Traverse Overview

The maximum speed throughout each assigned traverse segment was predicted, subject to the vehicle limits (acceleration, braking, handling and absorbed power). Below table shows the maximum and average vehicle speeds from Adams™ compared to physical test results.

Table 6-1: Traverse Maximum and average vehicle speed

Events	Average Speed (mph)		Maximum Speed (mph)	
	Test	ADAMS	Test	ADAMS
Y1	24.2	27.14	42.3	43.35
Y2	24.3	21.62	39.4	42.28
Y7	10.5	14.15	18.6	26.49
B2	13.1	17.9	26.6	31.85

In most cases, both the maximum and average speed obtained through Adams™ simulation was higher than obtained through physical test. This is to be expected due to several contributing factors:

- **Lack of Caution:** The model has no consequences due to failure. There is no risk to driver safety or equipment damage. Hence, the vehicle performance limits can be pushed and it is not necessary to account for terrain hazards, driver visibility, or uncertainty.
- **Optimization**: The modeling goal of maximum speed throughout each segment requires an iterative optimization approach. This should approach a "best-case" solution, subject to vehicle and terrain model assumptions.

- **Simplified Terramechanics Behavior**: The drawbar results indicate that the Bekker-Wong approach is prone to over-predicting traction on these soils. When applied to the traverse, this additional traction enables greater speeds.

There were also some factors observed that could contribute to reduced simulation speeds relative to test. The most prominent among these was inaccuracies in the terrain representation, due to vegetation contributions to the scanned "road surface." Though MSC's assigned terrain was relatively free of vegetation, for some sections vegetation contributions made the scanned surfaces used for simulation much more severe than the vehicle would experience in the corresponding test. In addition, there are some situations where driver awareness will result in improved performance relative to test. The optimization process may not avoid rocks, ruts, or similar small obstacles that a real driver can adjust for.

Hence, while it is clear that current simulation methods can yield very accurate performance predictions, the results shown here still require significant analyst involvement due to the optimization activities and multiple evaluation criteria required. Automating this level of prediction for applications similar to current NRMM use cases will require additional development in the areas of terrain processing and autonomous simulation logic.

Chapter 7 – Mobility Mapping

Eric Pesheck and Venkatesan Jeganathan
MSC Software Corporation, United States

In support of the Next Generation NATO Reference Mobility Model (NG-NRMM) Luciad Lightspeed technology was used to provide visualization of the KRC terrain and the associated FED Alpha vehicle's predicted mobility characteristics. The inputs to the mapping application included geospatial layers for soil type, elevation, grade, and aerial imagery. In addition, the vehicle capability (maximum speed) for various grades, and soil types, was generated through Adams™ simulations and provided in table format. Given this information, the application provides two mobility-focused capabilities:

- **Speed Made Good Map:** The soil, grade and vehicle performance data were combined to visualize the maximum vehicle speed throughout the map
- **Route Planning:** Given selected route endpoints, the application will compute an optimal cross-country route, along with elapsed time and distance traveled.

Luciad Lightspeed provides the foundations for advanced geospatial analytics applications. It allows users to rapidly develop high performance and location intelligence applications. Luciad Lightspeed's many software components and connectors allow users to fuse, visualize and analyze geospatial data. This can include static and moving data, maps, satellite imagery, crowd-sourced data, full motion video, weather data and terrain elevation in many different geodetic references and map projections.

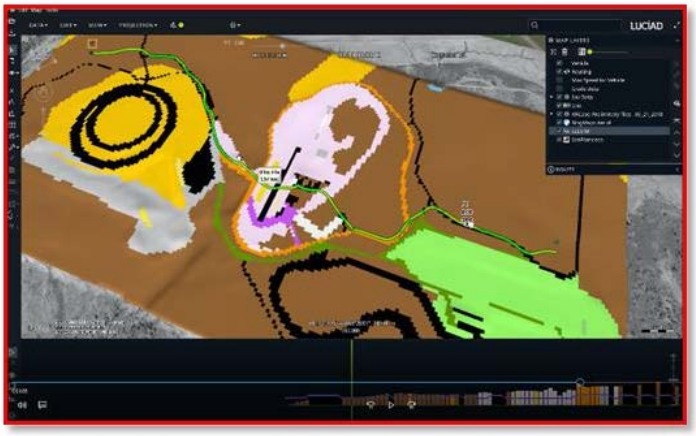

Figure 7-1: Luciad Lightspeed Application

7.1.Speed Made Good Maps

A framework for vehicle analysis methods accounting for the variability of the terrain and soil properties was successfully demonstrated in previous chapters using rigid roads as well as simple or complex terramechanics. This capability for evaluating the vehicle under multiple soil and grade conditions allows

broad characterization of the vehicle performance throughout a given terrain. Provided with terrain details, the vehicle properties can be projected onto a map to visualize the vehicle capabilities. This map, showing the maximum obtainable speed at each location is typically referred to as a Speed Made Good map. A map like this facilitates operational mission planning, as it can clearly indicate areas where soil or grade will contribute to or degrade vehicle mobility.

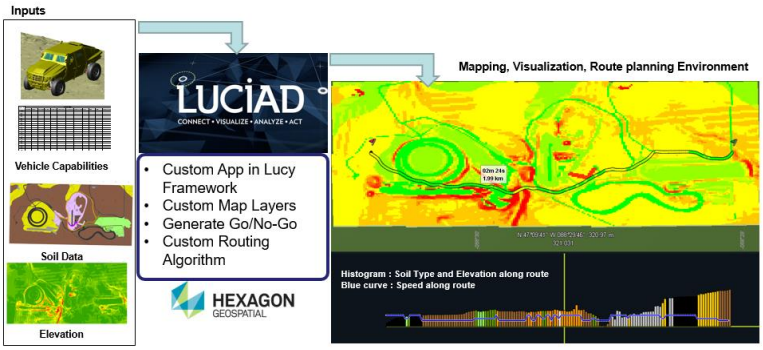

Figure 7-2: Mapping workflow, showing speed made good and route prediction results

The application developed for this project predicts an optimal route that accounts for both the soil and the effective grade along the path (e.g. traversing a slope is treated the same as flat). This tool has been developed to illustrate the capability of modern geospatial software in a mobility context and is not expected to provide a comprehensive mobility assessment. For effective operational use, it would be necessary to incorporate significant additional logic into the tool, including side-slope characteristics, RMS limitations, and obstacle information. Beyond this, the Luciad framework can facilitate integration of additional information such as line-of-sight considerations and real-time sensor inputs.

7.2. UQ and Stochastic Mobility Maps

The mobility maps discussed above (and all other model results so far) assume a deterministic representation of the world. In other words, there is an implicit assumption that all the model and terrain data is accurate. In reality, there is some level of uncertainty associated with all simulation and terrain inputs. The field of Uncertainty Quantification (UQ) is dedicated to understanding and analyzing the consequences of this natural variation. While UQ is not a focus of MSC Software, it is pertinent to the NG-NRMM mission, and both the Adams™ vehicle model and the Luciad mapping application were used to contribute to UQ-focused NG-NRMM activities.

For typical Adams™ results, some “average” ground property is assumed. This works well for typical performance prediction. However, when considering a geographical context, the statistical variation in terrain properties can become an important factor in mission planning. Without accounting for this, the deterministic approach may be excessively optimistic.

In support of the NG-NRMM UQ activities, MSC performed two specific tasks: UQ analysis support, and

Stochastic mapping. These are each described in additional detail below.

7.2.1. UQ Analysis Support

RAMDO Solutions was tasked with the determination of statistical terrain and soil models, based on the KRC soil test results, and available geospatial data. Based on these models, MSC was provided with several data sets corresponding to potential combinations of Bekker-Wong soil property coefficients and terrain grade. For each soil and grade, MSC generated a corresponding road and predicted a resultant maximum attainable vehicle speed. For cases where the grade was steep or predicted results were quite slow, the analysis was repeated in low gear with locked differentials to maximize power and traction. Over the course of the NG-NRMM analysis effort, several hundred simulation results were provided to RAMDO Solutions for use in their subsequent modeling activities. In general, these results were complicated by the fact that the individual soil parameter combinations did not always correspond to physically meaningful (or numerically stable) soil behavior.

7.2.2. Stochastic Mobility Maps

Given the vehicle performance predicted across a statistical range of soils and grades, a corresponding statistical representation of the vehicle capabilities could be developed. MSC worked with RAMDO solutions to populate the Luciad mapping application with statistical vehicle and terrain representations. This required generation of vehicle performance data corresponding to different levels of confidence, e.g. at some location, there is a 90% probability that the FED vehicle could go at least 37.41 kph on fine grain sand at a 10% grade, but there is a 20% chance that it could go at least 30.76 kph. In addition, revised elevation data was provided with different statistical confidence levels. Given this data, the application could be used to predict routes that account for uncertainty.

The maps shown below reflect confidence levels of 90% and 20%, with coloring that indicates the predicted speed made good. The map differences result in different optimal route solutions, given matching start and end points. The 20% route predicts a faster time, but there is only an estimated 20% chance that the vehicle could achieve this speed at any point along this route. In comparison, the 90% map indicates slower speeds, but the confidence of achieving this speed is much higher. Note that the source data for the stochastic maps shown here was generated by CM Labs, illustrating the "agnostic" nature of the Luciad framework.

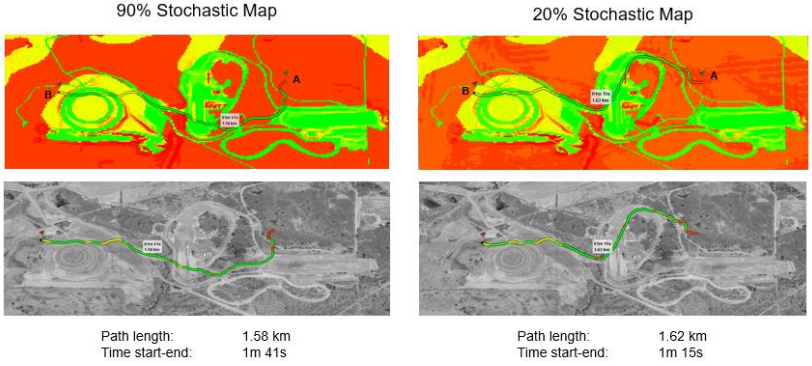

Figure 7-3: 90% and 20% Stochastic Maps

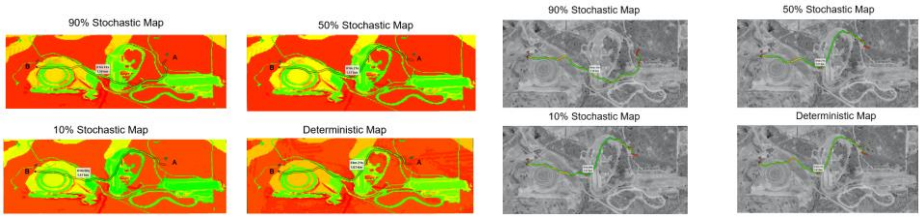

Figure 7-4: Stochastic and Deterministic Maps

As illustrated by the figures above, the Luciad Lightspeed technology has been successfully demonstrated for synthesizing data from the simulation and geospatial domains for effective visualization of vehicle mobility characteristics over specific terrain. In addition, through the incorporation of UQ analysis data, the methods may be extended to generation of stochastic mobility maps that facilitate additional operational confidence behind the Speed-Made-Good representation and resultant mission planning. Furthermore, the demonstrated framework may easily be expanded to incorporate additional terrain content, vehicle considerations, stochastic variations, or route optimization logic.

Chapter 8 - Real Time Virtual Model Performance

Eric Pesheck, Venkatesan Jeganathan, Paspuleti Rahul Naidu
MSC Software Corporation, United States

Finally, with autonomous vehicles on the horizon, MSC took advantage of the opportunity to highlight its latest capabilities in the area of real-time dynamic simulation. In this effort, a real-time version of the FED-Alpha vehicle dynamics model was created and verified against the original Adams™ model. In addition, to demonstrate these real-time capabilities, MSC installed this model on a Vires Virtual Test Drive (VTD) driving simulator, which was made available for CDT-participant review.

Real Time computational speed is a pre-requisite when combining software models with hardware components, such as a chassis stability controllers, vision / range sensors, Autonomous driving modules, or a driving simulator. MSC Adams™ has long been the automotive industry's tool of choice for high-fidelity vehicle dynamics predictions, but these models typically have not conformed to the strict protocols of Real-Time computation.

Now, with Adams™ Real Time, analysts can reuse the same base model for high fidelity integrated simulations, through SIL (Software-in-the-loop) to HIL (Hardware-in-the-loop) and ADAS (Advanced Driver Assistance Systems) applications. Typically, a unique variant of the original detailed model is developed that can meet the real-time requirements of the application of interest. This variant achieves a reduced order system while maximizing re-use of the existing validated model. This one tool-one model approach has the potential to remove weeks from the typical vehicle development program and save tens of thousands of dollars by eliminating the error-prone model translations between different tools. In addition, this approach does not dictate the model states or I/O channels, so it can be flexibly applied to a variety of vehicle development applications. Furthermore, the technology is not limited to vehicle applications. The Adams™ Real-Time solver may easily be applied to other MBD modeling disciplines, such as robotics or aerospace.

8.1. Adams™ Real Time Integrator:

The Real Time Integrator is an Adams™ solver approach that allows the user to meet specific real time operating system requirements. This Integrator ensures that both the Adams™ simulation speed and the communication interval meet the real time platform/hardware requirements (e.g. driving simulator, or ABS controller). Typically, a given application will have a known sampling rate at which the model is expected to exchange I/O information. Given this frequency, the analyst can adjust the Adams™ model content to achieve robust accurate performance, in real time, at the correct sampling interval. Typically, for vehicles, this is done through several strategies:

- **Idealize Connections:** A typical vehicle contains numerous bushings. While important for comfort and durability, many may be replaced by idealized constraints in order to simplify the system dynamics.
- **Simplify Components:** It is often possible to reduce computational time by replacing detailed component models with simpler representations. Common components that require reduced models are anti-roll bars, leaf springs, and tires.
- **Reduce solver file read-write:** Typically, for Real Time applications, it is not necessary to capture all of the model data associated with a typical Adams™ analysis, and the output channels can be

eliminated or greatly reduced.

The extent that these strategies must be employed, along with the selection of particular bushings, components, channels, etc. will depend on the application, sampling rate, and hardware involved. Though these decisions require analyst involvement, it also results in a highly flexible platform for integrating with real-time scenarios. Lastly, as hardware speeds advance, any requirements to sacrifice fidelity will gradually be relaxed.

For the FED-Alpha vehicle, the purpose was to demonstrate real-time solution capability while documenting the associated model accuracy. There is no particular targeted use-case for hardware or software integration that would help to dictate the required model fidelity or communication interval. For this case, the following modeling adjustments were made:

- **Kinematic Suspensions:** Given the typical stiffness of suspension bushings within a military vehicle, replacing these compliant connections with idealized rigid constraints is not likely to significantly degrade the model fidelity.
- **Reduced-order anti-roll bar (ARB):** The original model contained a beam-element based ARB. While accurate, this requires many degrees of freedom, while only slightly improving model accuracy. An equivalent two-part model was implemented.
- **Reduced I/O:** The model instrumentation content was somewhat reduced, although many channels were retained. The corresponding model results file sizes were typically reduced by 40%

As a consequence of the model changes, the FED model was reduced from 238 DOF, to 82 in the Real-Time model variant.

In order to retain consistency with all results previously generated, the Real Time FED model was run at the same output interval as each prior analysis. These varied from 100 to 1000 Hz, depending on the event. Given the variety of analysis scenarios, MSC's intent was to generate a model that could achieve real-time for most analysis scenarios, but not to exhaustively attempt to achieve real-time performance in all NG-NRMM analysis scenarios. When used, the Real Time integrator option reports an effective Real Time Index (RTI) that measures the effective ratio between the models solve speed and elapsed time. When the RTI is below 1, the model is running faster than real time on the specific hardware employed for the test. The table below summarizes the performance results for select events. For these events, a 2.8 GHz i7 4-core windows 10 laptop with 32GB of RAM running Adams™ 2018 was used.

The plots below summarize the results observed when the Real Time model results were compared against those from the validated full-vehicle model.

8.2. Real-Time Results comparison:

Since the description of the events are already provided in Chapters 3 and 4, only the plots with comparison of results from real-time model and the original model are compared here.

8.2.1. Acceleration

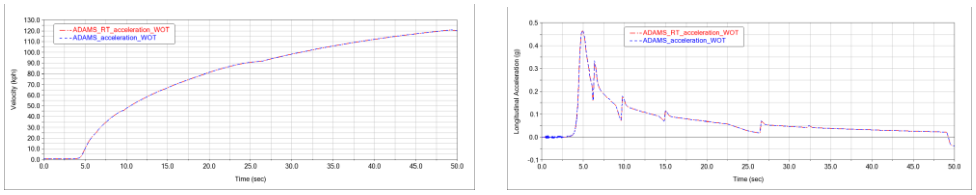

Figure 8-1: RT Acceleration: Vehicle speed and acceleration

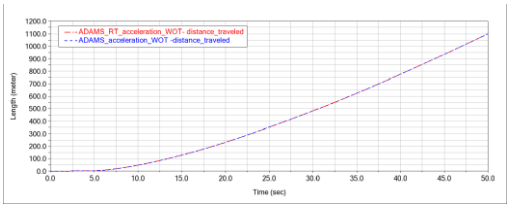

Figure 8-2: RT Acceleration: Distance travelled

8.2.2. Constant Radius Cornering

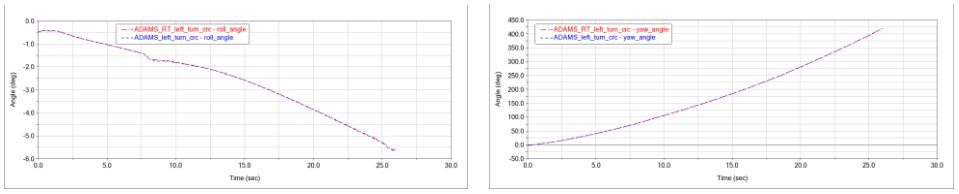

Figure 8-3: RT CRC : Roll Angle, Yaw angle

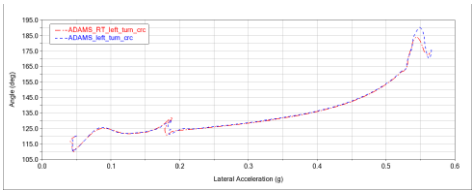

Figure 8-4: RT CRC : Steering wheel angle vs lateral acceleration

8.2.3. Double Lane change

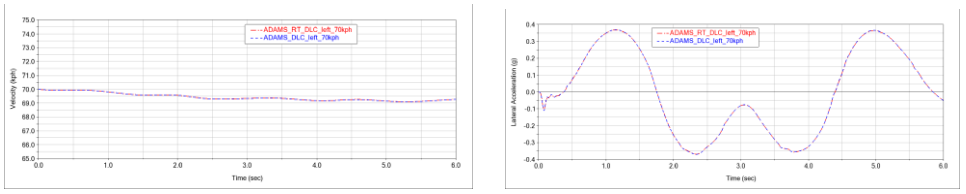

Figure 8-5: RT DLC : Vehicle Speed, Lateral Acceleration

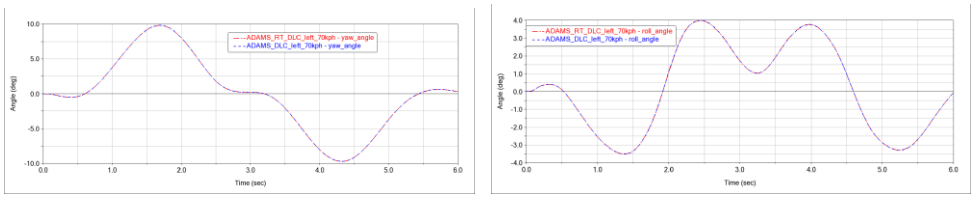

Figure 8-6: RT DLC : Yaw Angle, Roll Angle

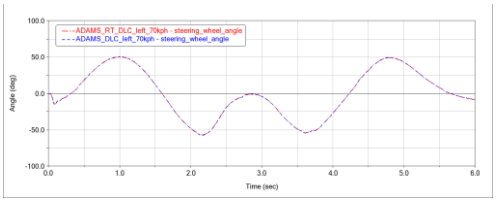

Figure 8-7: RT DLC: Steering Wheel Angle

8.2.4. Drawbar Pull

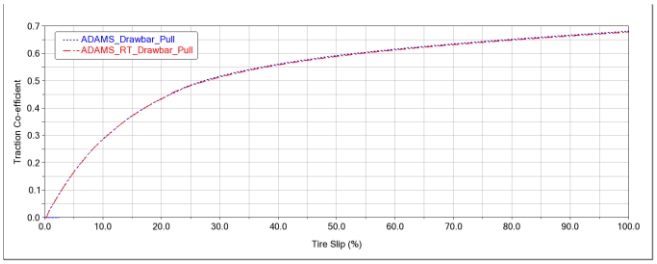

Figure 8-8: RT Drawbar pull : Traction co-efficient vs percent tire slip

8.2.5. Grade Climb

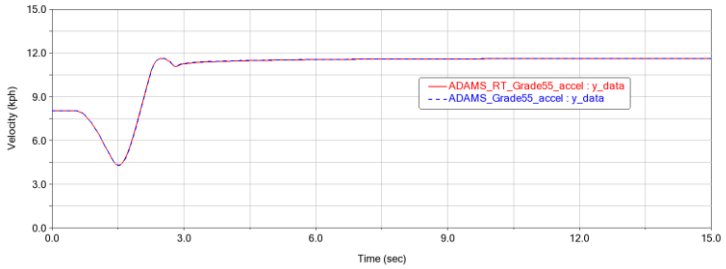

Figure 8-9: RT Grade Climb: Vehicle Speed

8.2.6. Half Round – 10 inch

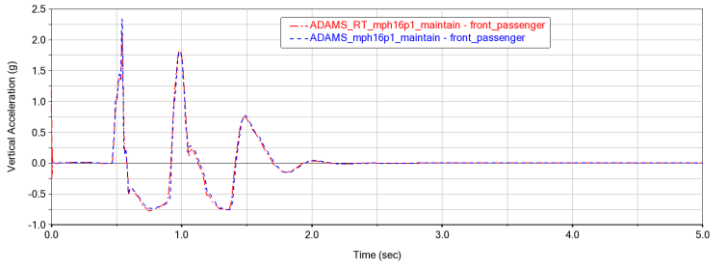

Figure 8-10: RT 10" half round : Seat Base Vertical Acceleration

8.2.7. RMS : 2 inch

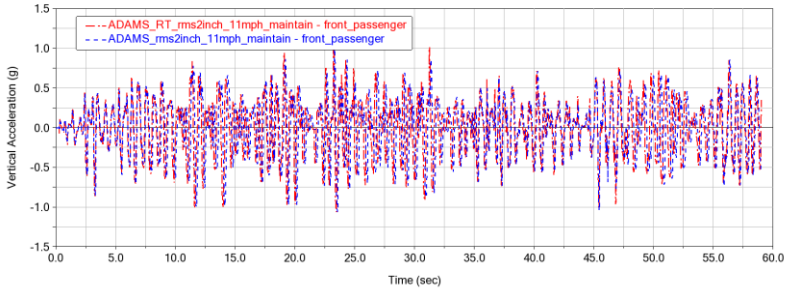

Figure 8-11: RT 2" RMS : Seat Base Vertical Acceleration

8.2.8. Mobility Traverse – Segment B2

Section Uphill: Compacted crushed rock **Section Downhill: 2NS Soft Soil**

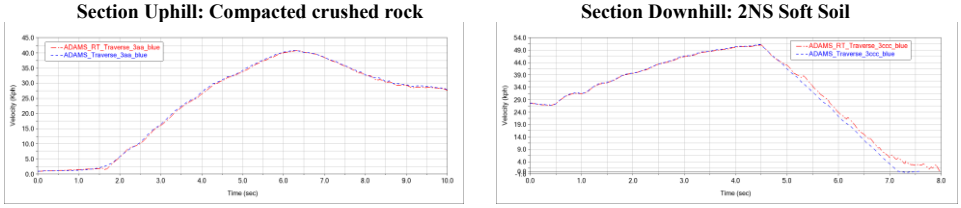

Figure 8-12: RT Mobility Traverse: Vehicle speed vs time

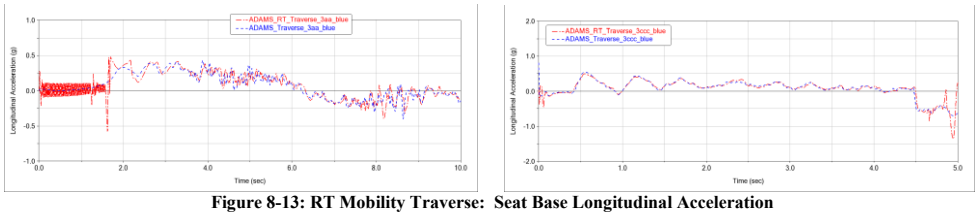

Figure 8-13: RT Mobility Traverse: Seat Base Longitudinal Acceleration

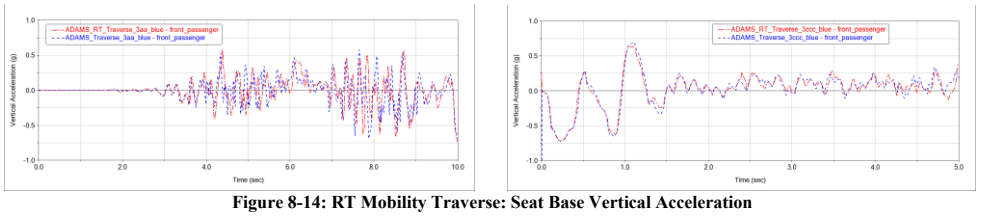

Figure 8-14: RT Mobility Traverse: Seat Base Vertical Acceleration

Figures 8-1 through 8-14 show a generally strong agreement between the real-time results and the original Adams™ solution. For smooth-road events, the events are essentially identical, indicating that a real-time approach is quite straight-forward with a few common-sense model adjustments. For the rough-road events, such as the 2-inch RMS and the traverse sections, more differences were observed. This indicates that some additional effort or different trade-offs might be necessary to retain accuracy in these scenarios. Recall that this study was performed using a common model for all events at the original event output step size. Achieving results agreement for some specific events might require finer integrator steps, different trade-offs within the model (i.e. less output, but more compliance and tire contact points). Detailed study of these trade-off options are outside the scope of this investigation.

8.3. Real-Time Index Summary:

Table 8-1: Real Time index for vehicle performance events

Event	Model Degrees of freedom	Real-Time Index(RTI)
Acceleration	82	0.18
Constant radius Cornering	82	0.16
Double Lane change	83	0.97
Drawbar Pull	90	0.49
Grade Climb	82	0.84
10" Half Round	78	1.31
2" RMS	78	0.59
Mobility Traverse - Crushed rock Terrain	78	0.93
Mobility Traverse - Soft soil	90	1.17

The table above summarizes the model performance with respect to real time for each of these events. Note that the changing system degrees of freedom are a result of changes to the tire, road and steering approaches among the different events. The half round and soft soil mobility traverse events show RTI index greater than 1 here. This does not necessarily indicate an inability to use the model for real time simulation of these scenarios. In addition to the model tuning approaches discussed earlier, employing a high performance computer (ex. 2.7 GHz 24 cores 64GB memory Red Hawk Linux) would be expected to yield improved analysis speeds. The methods, equipment, and compromises necessary to succeed with real-time methods are dependent on the associated model, application, and simulation event. However, the results shown here indicate that most mobility applications are well within reach of this capability, even with a complex, detailed, vehicle model.

Chapter 9 - Gaps

Eric Pesheck, Tony Bromwell
MSC Software Corporation, United States

While the NG-NRMM analysis effort was largely successful, it is incumbent on the participants to assess the entirety of the effort and identify areas that fell short of the goal in one way or another. Here, these gaps are summarized with respect to the vehicle modeling, soil modeling, and terrain representation.

For the vehicle model, it appears that the technology is really quite mature. Most vehicle-focused aspects of the effort may be well-represented using existing methods, and MSC's longstanding strength in modeling and simulating vehicles makes implementation of most vehicle behavior quite straight-forward. Correlation gaps in this area are most likely related to unavailable data, such as more detailed tire models, strut friction specifications, or body compliance. These reflect limitations in this particular case, but are not systemic limitations. As it is, the rigid-road events generally showed quite good agreement with test results.

The soil modeling and analysis process did expose several issues. The simplified terramechanics simulations generally showed fairly poor agreement with the test results. As most CAE vendors generated similar results, this weakness appears to be driven mostly by either poor agreement between Bekker-Wong theory and practice or by a test process that did not effectively evaluate the soil behaviors at the dimensions and loads experienced in the vehicle scenarios. In addition to the results quality, some opportunities for process improvement were also identified. It would be advantageous for MSC to enable mixed hard/soft surfaces or multiple soft surfaces within a single road to facilitate simulation over more complex terrains with variable surface characteristics. Beyond this, some additional Adams™ soft-soil road related integrator process and stability issues have been identified for further internal MSC investigation.

Although the end product of the EDEM-based complex terramechanics analyses was quite good, the effort did expose several significant concerns. First, the field of complex terramechanics is still developing, and there is clearly significant work to be done to reach consensus on 'best practice' methods. It remains difficult to adjust properties at the particle level in order to achieve targeted bulk material characteristics. In addition, there are no established processes for scaling particle size while maintaining consistent bulk properties. This issue overlaps with the high computational efforts associated with DEM methods in that computation issues force the particle sizes to be quite large when performing vehicle simulation, but replicating in-situ soil testing with these same large particles is not ideal. Lastly, while MSC has facilitated EDEM cosimulation by the incorporation of some specific analytical methods and interface tools, MSC has identified several opportunities to improve the associated modeling and simulation process.

Lastly, over the course of this effort it became clear that there is a gap between road-focused surface representations and more general-purpose terrain representations. There are several different standards and methods in place for specifying and using road surfaces throughout the global automotive simulation community. These methods are typically focused on specifying a detailed surface along some ribbon-like road path, and are well suited for evaluating vehicle ride quality or internal loads along this road. These methods facilitate evaluation of absorbed power over RMS roads, or the vehicle response to obstacles such as halfrounds, ditches and steps. However, the automotive simulation community (as well as MSC, specifically) does not have clear standards, methods, or processes in place to facilitate the creation of large-scale terrain for use in off-road simulation based on scanned terrain data. In addition, most industry simulation tools do not allow road surfaces to contain multiple soil representations, beyond simple changes to the surface friction.

There is a general need to facilitate interaction between the mapping and simulation communities to facilitate more direct use of existing geospatial surface representations within simulation. In addition, this could include leveraging additional underlying geographic data layers, such as soil definitions or moisture content. Implementation of more general terrain capabilities implies the need for more free-form driving through this area, which then may require additional driver control options or some autonomous capability to interpret the terrain. Similarly, when the Adams™ Real Time model was integrated with the VTD simulator and test environment, it was not possible in the time available to integrate the KRC terrain representation and allow the driver to roam the KRC grounds. There are significant opportunities for improvement in this area.

Beyond the ability to easily implement scanned surface representations, there are separate issues associated with the data-processing of this scanned data for the development of appropriate surfaces for simulation. Within this project, there were numerous issues with "noise" in the scanned surfaces due to vegetation. If not addressed, this makes the terrain unrealistically harsh. Processes should be developed that facilitate more effective filtering/smoothing of the scanned data to remove this noise, or scanners should recognize and eliminate the undesired content.

While some of the gaps above point to areas that may be addressed by MSC to yield a more efficient and accurate modeling and simulation process, most point to larger issues that extend outside MSC's domain. Specifically, it appears that significant contributions could be made by additional fundamental research in both the simplified and complex terramechanics disciplines. In addition, alignment between the terrain and road communities (or at least some clear standards for representing terrain for simulation) would be most effective if led by the end-user organizations. Given some standard, MSC can work toward implementation.

Chapter 10 – Path Forward

Eric Pesheck, Tony Bromwell
MSC Software Corporation, United States

The existing NRMM program contains a rich and noble history that has been developed over decades of research and in-service application. It has proven its worth and value numerous times and is a important tool for mission planners. However, throughout its application it has also provided insight into its limitations. While it cannot be said that we now have all the answers, vehicle development, geospatial sensing, vehicle simulation technology and computer science have evolved considerably since the NRMM's initial development. The results of this project clearly demonstrate that the NRMM should be enhanced to include these industry-proven technologies to not only ensure more successful mission planning, but for enhanced warfighter safety. Furthermore, as demonstrated herein, there is the potential for making the NG-NRMM a tool that could be used in real-time, in the vehicle, by the warfighter in a dynamic environment to provide a quantum leap in applicability and effectiveness.

The goal of this project was to determine the degree that current vehicle simulation software codes, along with UQ metrics, could enhance mobility predictions beyond the performance of the current NRMM toolset. The results of the work outlined here achieve this goal and clearly provide a higher level of fidelity for predicting a vehicle's ability to traverse various terrains and soil types. Combining these simulation results with UQ methods results provides a significantly higher level of confidence in not only mobility but also success for any new mission planning.

Furthermore, from the additional work performed by MSC in demonstrating their Real Time solver capabilities along with the introduction of the Luciad Litespeed software application, the results of this work provide a line of sight to the potential for delivering a Mobility Mapping System directly to the warfighter - in theater, in vehicle. Achieving this goal will provide the ultimate benefit.

However, there is a lot of work to be done to achieve this ultimate goal. The path forward has several potential branches. Based on MSC's perspective we recommend the following activities:

- **NATO StanAg & StanRec**: MSC is interested in supporting the work associated with the process of developing NATO StanAg and StanRec documents to define applicable model/terrain/soil/methods standards that are well-suited for future mobility analysis efforts.
- **Product Gaps**: MSC will review and incorporate product capability gaps into our future product planning (subject to corporate priority).
- **Terramechanics**: MSC is willing to cooperate with initiatives to evaluate progress in both simplified and complex terramechanics for improved mobility prediction.
- **Vehicle Performance Database**: MSC is interested in working with NATO defense agencies to populate existing vehicle performance data necessary to support an NG-NRMM deployment.
- **New Vehicle Development**: MSC is interested in working with NATO defense agencies and defense contractors in the development of new vehicles for both enhanced mobility capabilities as well as populating the performance dataset necessary for use with an NG-NRMM deployment.
- **Proof of Concept**: MSC is interested in working with NATO defense agencies for developing a proof

of concept for advanced mobility mapping applications for both operational planning and in-vehicle use.

10.1. NATO STANAG & STANREC

It is understood that to formalize the results of the work contained herein, the results need to be turned into a STANAG or STANREC that NATO can formally adopt. MSC is interested in supporting this work via participation on committees dedicated to this effort.

a. NATO Standardization Agreement (STANAG)

A STANAG is a normative document that records an agreement among several or all NATO member states – ratified at the authorized national level – to implement a standard, in whole or in part, with or without reservation.

b. NATO Standardization Recommendation (STANREC)

A STANREC is a non-binding document employed on a voluntary basis and does not require commitment of the Nations to implement the standards which are listed in it.

10.2. Product Gaps

As was noted, in the previous chapter, the work conducted herein identified a series of gaps that require further study. It is recommended that formal work be initiated to study, minimize and eliminate these gaps. This work can be done individually or through a combination of research by government, industry and academia. MSC will identify gaps within its control and will discuss them with our product planning group. Request for new product features come from multiple sources in multiple industries and require prioritization with our business strategy and funding allocations. Therefore, we cannot commit to any definitive technology advancement or schedule at this time.

10.3. Terramechanics

Much of the unknowns and uncertainties presented throughout this report can be attributed to terramechanics, both simple and complex. Additionally, it was clear from the simulation results that complex terramechanics can provide greater fidelity and insight in certain situations. Given this information, additional research is recommend in this area.

With respect to the vehicle performance in off-road situations, a lot of the fidelity and unknowns can be attributed to the tire model and the tire-soil interaction. These are areas of recommended future research. A higher performing Ftire model would help in several situations that have been previously documented. MSC has extensive experience with this type of model and can assist with the tire testing, characterization, modelling and simulation using this model.

Additionally, from the results of the DEM modelling that was conducted it was clear that further work in this area is required. A better understanding of the soil properties along with a better understanding of how the various tire treads interact with the soil types would provide a huge benefit to better predicting the vehicles performance in off-road situations and conditions. Continued work with EDEM in this area is recommended.

Finally, as mentioned, the complex terramechanics models tend to provide a higher level of fidelity in soft soil conditions. However, this method is computationally expensive and in certain situations unfeasible for use. It is recommended that future research be focused on using complex terramechanics models to enhance the understanding and fidelity of the tire-soil interaction, such that these results can be transferred into a simple terramechanics model that can be used effectively and efficiently in an NG-NRMM model.

10.4. Vehicle Performance Database

For NATO countries and defence agencies to effectively use an NG-NRMM tool significant information will be required for the subject vehicles. Similar to the work conducted and documented herein, each vehicle will require a validated simulation model along with a performance dataset that can be incorporated into the NG-NRMM tool. This dataset will contain the results of multiple simulation events in an effort to provide a holistic overview of vehicle performance on a variety of terrains, soil types, speeds, grades, loading, tires, etc.

MSC has proven its ability to provide the highest level of fidelity and accuracy for such data as clearly presented herein. We would like to continue this work by partnering with the various NATO countries and defence agencies in developing vehicle performance datasets any vehicle of interest.

The MSC Global Engineering Services organization is comprised of a team of engineers and scientists with expertise across a wide range of engineering disciplines and industries. MSC has a history of over 50 years of real world, hands-on practical experience. We are backed by a world-class suite of software and direct access to the software product development team.

10.5. New Vehicle Development

As alluded to above, MSC has a broad and extensive vehicle dynamics development resume for both wheeled and tracked vehicles including personal and commercial automotive vehicles, recreational vehicles, and defence vehicles. Leveraging our software and vehicle development experience we are a recognized leader in this field and are interested in partnering with any NATO country, defence agency or defence contractor in assisting with new vehicle development programs.

MSC can assist with traditional vehicle dynamics development for better ride and handling performance as well as developments for improved mobility under a variety of conditions. Furthermore, the results of this work can provide the dataset needed for incorporation into an NG-NRMM model.

10.6. Proof of Concept

The results of this study provide clear evidence that the NG-NRMM model is both feasible and beneficial. Furthermore, it is believed that there was enough evidence to prove that the NG-NRMM models may be leveraged for both remote logistics and operational mission planning as well as a hand-held mobile toolset - one that could be deployed in theater with the warfighter and used interactively throughout the mission. The benefits of either of these objectives are significant.

MSC would be interested in working with its sister company Luciad along with NATO defense agencies in the development of a working proof-of-concept (POC) for either of these two objectives. Leveraging the MSC Adams Real Time solver along with known or entered vehicle data, mobility calculations could be conducted on-demand. These results would integrate with or replace previously

calculated performance data to provide real-world, real-time mobility information. Integrating these results with the Luciad Litespeed technology could provide enhanced mobility information and route planning to the warfighter in theater. Additionally, the added benefits the Luciad technology provides, such as line of sight, could be integrated into the routing logic to future enhance warfighter stealth and safety.

Chapter 11 - Conclusion

Eric Pesheck
MSC Software Corporation, United States

The NG-NRMM effort has been focused on the evaluation of existing and emerging technologies for improving upon the current capabilities of the long-standing NRMM toolset. As documented in this report, MSC has contributed to this assessment in the areas of:

- Vehicle model fidelity
- Simplified terramechanics
- Complex terramechanics
- Operational performance prediction
- Mobility mapping and route planning
- Real-time simulation

Advances in multi-body dynamics (MBD) CAE tools such as Adams™ allow vehicle models to be very precise, and generate accurate performance predictions. These models can incorporate very general suspension arrangements and topologies, while also allowing for the incorporation of advanced technologies such as active suspensions or the frequency selective damper used in the FED-Alpha vehicle. In addition, the detail of modern post-processing capability allows detailed evaluation of vehicle clearance properties. These capabilities were clearly illustrated by the modeling process described in Chapter 2 and the results presented in Chapters 3 and 4. The demonstrated accuracy and capability, while not pushing the limits of current CAE methods, still significantly exceed that of the current NRMM tool. These results make a clear case for the incorporation of MBD modeling and simulation tools into the NG-NRMM framework.

The existing theory underlying simplified terramechanics as well as the collection and identification of associated parameters contain numerous assumptions that complicate its application within the NG-NRMM framework. This was illustrated by the uneven results obtained in this study. The results generally over predicted available traction, although some predictions were closer (FGS-wet in Chapter 3) than others (CGS and FGS-Dry in Chapter 5). The fundamental issues underlying this inaccuracy remain uncertain. However, roughly similar simplified terramechanics results across CAE vendors point to generally consistent application of the existing theory. MSC analysis tools have demonstrated capability for assessing the vehicle in a soft-soil environment and given revised input parameters or formulation, the existing approach should generate applicable mobility predictions.

Similarly, analysis via the complex terramechanics approach showed promise but was not without its complications. The results presented here, using a coupled simulation between Adams™ and EDEM (see Chapter 5) correlated quite well to test, and indicate promise for the DEM approach. However, the process of defining appropriate particle properties, the high computational costs of the approach, and the added complexity of implementing a co-simulation contribute to the difficulty and inefficiency of using this analysis approach. As the field of DEM matures and computational capability improves, the DEM approach to complex terramechanics is likely to become increasingly attractive.

The core concern of mobility is to predict operational capability in the field. Within this project, the most direct assessment of this was the mobility traverse performed at KRC. The traverse directly evaluates

the performance of the vehicle in a variety of challenging scenarios, and allows the most direct comparison to operational performance metrics and existing NRMM methods. Adams™ Car was able to effectively simulate the vehicle performance over several assigned traverse sections (see Chapter 6) including rigid road, simplified terramechanics, and complex terramechanics surfaces, effectively incorporating vehicle acceleration, braking, traction, and cornering limits. As a result, the predicted vehicle speed and resulting traverse elapsed time accurately compare against the in-field results. This outcome is indicative of the high potential operational value that may be obtained when advances in MBD, terramechanics, and terrain processing are applied to specific mobility scenarios.

The extension from the specific routes defining the mobility traverse to a more generalized mapping environment was illustrated in Chapter 7. Along with the advances in the fields of MBD and terramechanics, there have been major changes in the geospatial technology field. The amount of potential data that can be accumulated and presented for any given terrain has grown by orders of magnitude, and the toolsets that have developed in support of this growth can be leveraged to great effect for mobility assessment. Luciad's capabilities in this area were illustrated through the development of a custom application that effectively combined the available terrain data with predicted vehicle capability to generate "Speed made good" maps and optimal travel routes throughout the KRC test facility. This tool illustrates the power of leveraging existing geospatial platforms to effectively combine performance data with detailed geographical information to provide effective operational tools. Clearly, as the available geospatial data multiplies, both the opportunity for using this data and the necessity for associated visualization tools will grow as well.

Beyond the concerns listed above, there are ongoing needs to leverage simulation models for a broad array of Real-Time scenarios, ranging from simulator applications to integrated hardware development (HiL). The ability to use a validated mobility model in these scenarios without significant additional translation and validation activities can improve process efficiency for many organizations. Within this project, MSC illustrated that a Real-Time variant of the validated vehicle model could perform nearly all of the evaluation events at real-time, and with minimal degradation of analysis results. This paves the way for further use of Real-Time solution methods, without the simplifications or topology restrictions imposed by many commercial real-time vehicle simulation tools.

As a whole, the NG-NRMM project posed many questions to the vehicle mobility community regarding the maturity and applicability of the contributing methods and technologies. Throughout this process, MSC has succeeded in incorporating these methods into our analyses and helping to generate quantitative answers to these questions. As a consequence of this, MSC has gained confidence in many vehicle modeling and analysis capabilities and their value to the mobility community. In addition, it has provided invaluable feedback to guide future development, validate development initiatives, and improve the functionality of existing features.